Renormalization group approach in Newtonian cosmology

Yasuhide Sota,* Toshiyuki Kobayashi,† and Kei-ichi Maeda‡
Department of Physics, Waseda University, 3-4-1 Okubo, Shinjuku-ku, Tokyo 169, Japan

Tomomi Kurokawa§ and Masahiro Morikawa‖
Department of Physics, Ochanomizu University, 1-1 Otuka, 2 Bunkyo-ku, Tokyo 112, Japan

Akika Nakamichi¶
Gunma Astronomical Observatory, 1-18-7 Ohtomo, Maebashi, Gunma 371, Japan
(Received 26 January 1998; published 30 June 1998)

We apply the renormalization group (RG) method to examine the observable scaling properties in Newtonian cosmology. The original scaling properties of the equations of motion in our model are modified for averaged observables on constant time slices. In the RG flow diagram, we find three robust fixed points: Einstein–de Sitter, Milne, and quiescent fixed points. Their stability (or instability) property does not change under the effect of fluctuations. Inspired by the inflationary scenario in the early Universe, we set the Einstein–de Sitter fixed point with small fluctuations as the boundary condition at the horizon scale. Solving the RG equations under this boundary condition toward the smaller scales, we find a generic behavior of observables such that the density parameter Ω decreases, while the Hubble parameter H increases for a smaller averaging volume. The quantitative scaling properties are analyzed by calculating the characteristic exponents around each fixed point. Finally we argue the possible fractal structure of the Universe beyond the horizon scale. [S0556-2821(98)05714-2]

PACS number(s): 98.80.Hw, 11.10.Hi

I. INTRODUCTION

Several pieces of observational evidence imply scaling properties in the present Universe. For example, (a) de Vaucouleurs compiled data of a density-size relation for galaxies and clusters of galaxies, and pointed out the scaling relation of $\ln \rho = -1.7 \ln L$, where L is the linear scale of each astrophysical object and ρ is the mass density averaged at this scale [1]. This relation asserts the systematic decrease of the density at a larger scale. (b) It is widely known that the observed two-point correlation function $\xi(r)$ for galaxies or for clusters has the scaling property $\xi(r) \propto r^{-1.8}$ [2]. (c) Pietronero and his collaborators discuss a fractal structure of the Universe and claim that the fractal dimension is about two up to the scale of 1000 Mpc [3]. (d) The observations of the mass-luminosity ratio for the various astronomical objects linearly increases toward the larger scale up to a scale of about 10 Mpc [4].

Motivated by the above pieces of observational evidence, we explore systematic underlying physics which may govern the scaling properties of observables in the present Universe. Usually the above scaling properties are understood as a result of an interplay of the scale invariant initial condition (Harrison-Zel'dovich spectrum) and the gravitational instability [2]. In this usual approach, a global uniform background is assumed. In our approach, we do *not* assume such uniform background *a priori* but consider general inhomogeneous distributions.

Let us consider the scaling properties carefully. We start our analysis with the equations of motion for fluid in the Newtonian Universe neglecting the pressure term for simplicity. This set of equations admits a naive scale invariance; a scaling of space-time coordinates as well as an appropriate scaling of observables leaves the set of equations unchanged. We define this naive scaling transformation as the operation S. Such a naive scaling property is, however, not necessarily reflected in the actual observations in a direct form. This is because in general the physically measurable quantities are strongly affected by the actual method of observations. Therefore the above naive scaling should be modified when we apply it to the actual observations. There are at least two important factors for the modification: (1) An observable region is limited by causality, (2) we may merely observe averaged quantities in a certain region in space.

We first consider the factor (1). Actually, we can only observe a light signal from a galaxy located on our past light cone. In Newtonian cosmology, the observable quantities are located on a hyperslice of constant time. Because in general the above naive scale transformation also requires a change of the time variable, we have to adjust it so that we can compare the observable quantities with different scales on the same time slice. This adjustment can be implemented by the time evolution of the observables by using the equations of motion for them. We define this adjustment as the operation T. In this context, we have to reconsider exactly what we are measuring. In this paper we consider scaling behavior of the cosmological parameters. For example, the density parameter Ω is a dimensionless quantity and therefore it is

*Email: sota@gravity.phys.waseda.ac.jp
†Email: kobayasi@gravity.phys.waseda.ac.jp
‡Email: maeda@gravity.phys.waseda.ac.jp
§Email: tk385@phys.ocha.ac.jp
‖Email: hiro@phys.ocha.ac.jp
¶Email: akika@astron.pRef. gunma.jp

invariant under the naive scale transformation. However in many cases, we can directly measure the matter density ρ and separately the cosmic expansion parameter H [5]. The combination of these observations *induces* the value of the density parameter Ω [6] which depends on the scale. In this case, the scale transformation and the necessary time adjustment are nontrivial. Thus we have to carefully distinguish the direct observables and the secondary *induced* observables.

Next we consider factor (2). What we observe is necessarily an averaged quantity on some region of space-time because there are always spatial fluctuations and the resolution of our observation is limited. Therefore the observables are most generally dependent on the scale of averaging. We define this averaging as the operation A. However, it would be very difficult to consider the invariant averaging procedure in the full general relativity and to make connection with observables [7]. Therefore, mainly because of this reason it would be better to restrict our considerations to the Newtonian cosmology, in which an averaging procedure is properly defined and is explicitly calculated [8].

After the above adjustments (1) the operation T and (2) the operation A on the original naive scaling properties of the underlying equations of motion, we would obtain the relevant information for actually observable quantities. Thus in general, the difference of two observables at different scales would be related with each other by the naive scaling (operation S) compensating time evolution (operation T) and the inevitable averaging procedure (operation A).

In order to unify the above operations S, T, and A, we need to introduce one more ingredient in our considerations. The most sophisticated method so far to deal with such multiple operations would be the renormalization group (RG) method [9]. This is a very general method to obtain the observable response of the system against the scale change and is widely used in various fields in physics including quantum field theory, statistical mechanics, fluid mechanics, etc. For example, in quantum field theory, a naive scaling in classical theory should be modified by the quantum fluctuations. In statistical physics, the scaling property is used with the averaging operation to yield critical exponents.

In this paper, we try to apply this RG method to Newtonian cosmology. In this model, the scaling invariance holds all the time. Thanks to the averaging procedure, we can define classical fluctuations of the observables. Then, naive scaling behaviors of the observables are modified by renormalization of the classical fluctuations. This is conceptually the same as RG methods in other fields of physics.

The RG equations we obtain give the effective scale change of averaged observables, and the effect of spatial fluctuations on observables. The flow diagram generated by the RG equations in the parameter space of observables represents how the observables actually change under the scale transformation. Each flow line represents a single physical system, in which the averaged variable at different scale corresponds to each point on the flow. Thus the RG flow gives a whole set of possible cosmological models. The fixed points, i.e., the stagnation points in the flow diagram, of the RG equations represent the possible ''uniform'' structure of observables, that is, the averaged variables do not depend on the scale and characterize diversities of the system.

There have been some applications of the RG method in cosmology [10]. The RG method is an effective tool to examine the asymptotic behavior of a dynamical system. In fact, Koike, Hara, and Adachi succeeded in explaining the critical behavior of a self-similar solution during the gravitational collapse of a radiation fluid using the RG method [11]. Subsequent series of studies are in this line of study [12]. In their cases, the aspects of (S) and (T) are reflected in their method. Thus their RG method does not necessarily contain an averaging procedure (A). On the other hand, Carfora and Marzuoli [13] and Carfora and Piotrkowska [14] explicitly accounted for the spatial fluctuation of physical quantities in general relativity and derived the RG equation reflecting the aspects (S) and (A). Since they concentrated on the scaling in the spatial direction, the aspect (T) has not been manifestly reflected in their approach. Here in this paper, to examine the scale dependence of the observables on a constant hyperslice, we apply the RG method from the full aspects of (S), (T), and (A) altogether, assuming some scaling property in averaging observables.

This paper is constructed as follows. In Sec. II, we derive the RG equation for the averaged Newtonian fluid. Section III is the main part of our analysis. Here we examine the RG flow in the parameter space and show that there appear three robust fixed points including the Einstein–de Sitter universe. We examine the effects of shear, tidal force, and fluctuations, and derive the scale dependence of the physical variables such as Ω and H around the Einstein–de Sitter universe. In Sec. IV, we summarize our results. We also present the full RG equations including fluctuations up to the second order cumulants in the Appendix.

II. DERIVATION OF RENORMALIZATION GROUP EQUATIONS

In Newtonian cosmology, the following equations describe the evolution of a self-gravitating fluid in the Eulerian coordinate system:

$$\frac{\partial \rho}{\partial t} = -\nabla \cdot (\rho \boldsymbol{v}),$$

$$\frac{\partial \boldsymbol{v}}{\partial t} = -(\boldsymbol{v} \cdot \nabla)\boldsymbol{v} + \boldsymbol{g},$$

$$\nabla \cdot \boldsymbol{g} = -4\pi G \rho, \tag{2.1}$$

where ρ, $\boldsymbol{v}$, and $\boldsymbol{g}(\equiv -\nabla\phi)$, respectively, denote the mass density, the velocity of the fluid, and the gravitational acceleration. Now we transform these equations into the Lagrangian coordinate system. In order to eliminate the gravitational acceleration $\boldsymbol{g}$, we introduce the spatial derivative of the velocity field and decompose it into a trace part (expansion $\theta = \nabla \cdot \boldsymbol{v}$), a symmetric traceless part (shear σ^i_j), and an antisymmetric part (rotation $\omega^i{}_j$) [8]. Then the above equations become

$$\frac{d\rho}{dt} = -\rho\theta, \tag{2.2}$$

$$\frac{d\theta}{dt} = -\frac{1}{3}\theta^2 + 2(\omega^2 - \sigma^2) - 4\pi G\rho, \tag{2.3}$$

$$\frac{d\sigma^i_j}{dt} = -\frac{2}{3}\theta\sigma^i{}_j - \sigma^i{}_k\sigma^k{}_j - \omega^i{}_k\omega^k{}_j + \frac{2}{3}(\sigma^2 - \omega^2)\delta^i{}_j - E^i_j, \tag{2.4}$$

$$\frac{d\omega^i{}_j}{dt} = -\frac{2}{3}\theta\omega^i{}_j - \sigma^i{}_k\omega^k{}_j - \omega^i{}_k\sigma^k{}_j, \tag{2.5}$$

where the Lagrange full time derivative

$$\frac{d}{dt} \equiv \frac{\partial}{\partial t} + \boldsymbol{v}\cdot\nabla \tag{2.6}$$

is used on the left-hand side. In these equations, σ and ω denote the magnitudes of shear and rotation, respectively, defined by

$$\sigma^2 = \frac{1}{2}\sigma^i{}_j\sigma^i{}_j \quad \text{and} \quad \omega^2 = \frac{1}{2}\omega^j{}_i\omega^i{}_j. \tag{2.7}$$

The tensor $E^j{}_i = \nabla^i\nabla_j\phi - \delta^j{}_i\nabla^2\phi/3$ denotes the tidal force which comes from the spatial difference of the gravitational acceleration. In pure Newtonian dynamics, this is a slaving variable and there is no equation of motion for it. Fortunately, several excellent approximation schemes have been developed to deal with this highly nonlocal quantity. In this paper, we mainly follow the local tidal approximation (LTA) [15–17] in which the equation of motion for the tensor E^i_j is given by

$$\frac{dE^j{}_i}{dt} = -\theta E^j{}_i - 4\pi G\rho\sigma^j{}_i. \tag{2.8}$$

Hereafter we neglect the rotation for simplicity ($\omega^j{}_i = 0$). Actually the initial assumption of $\omega^j{}_i = 0$ is sufficient to guarantee this condition all the time as is seen from the above equation. Thus irrotational motions form a closed subclass of the full dynamics. Then, we can simultaneously diagonalize both the matrices $\sigma^j{}_i$ and $E^j{}_i$. We work in the frame where they are diagonalized as σ_i and E_i ($i = 1,2,3$), respectively. Since $\sigma^j{}_i$ and $E^j{}_i$ are traceless, only the two components of each are independent. Then it may sometimes be more convenient to introduce the following variables $\sigma_\pm$ and $E_\pm$:

$$(\sigma_1, \sigma_2, \sigma_3) = (\sigma_+ + \sqrt{3}\sigma_-, \sigma_+ - \sqrt{3}\sigma_-, -2\sigma_+),$$
$$(E_1, E_2, E_3) = (E_+ + \sqrt{3}E_-, E_+ - \sqrt{3}E_-, -2E_+). \tag{2.9}$$

At a glance, we observe a scaling property in the above set of equations of motion (2.2)–(2.5), (2.8). They are invariant under the following scaling transformation:

$$t \to t' \equiv e^{s\Delta\tau}t,$$
$$\boldsymbol{x} \to \boldsymbol{x}' \equiv e^{\Delta\tau}\boldsymbol{x},$$
$$\theta \to \theta' \equiv e^{-s\Delta\tau}\theta,$$
$$\sigma_\pm \to \sigma'_\pm \equiv e^{-s\Delta\tau}\sigma_\pm,$$
$$E_\pm \to E'_\pm \equiv e^{-s\Delta\tau}E_\pm,$$
$$\rho \to \rho' \equiv e^{-2s\Delta\tau}\rho, \tag{2.10}$$

where s is a constant free parameter and $\Delta\tau = \tau' - \tau$ measures a change of scale.

Now, based on these scaling properties, we derive renormalization group equations for spatially averaged observables on a constant time slice. To analyze the structure of the Universe, we adopt a scaling solution of our basic equations. Such a scaling solution could be realized as a result of a self-gravitating dynamical system with a scale invariant density fluctuation [2], although here we do not specify any models to give such a scaling solution. If, however, we consider a scaling solution such as Eq. (2.10) as it is, we find either a homogeneous Universe or inhomogeneous Universe with a ''center,'' which is not consistent with the cosmological principle. We are interested in the inhomogeneous Universe model consistent with the cosmological principle such as a fractal universe. If we have a fractal universe, we expect that some averaged values around an observer may show a scaling property. Such a scaling property will be always observed anywhere because of a fractal structure of the Universe, which is consistent with the cosmological principle. This is why we consider spatially averaged observables here. We assume a scaling property such as Eq. (2.10) not only for averaged values of the variables in the above equations but also for those of the fluctuations such as a second order cumulant.

We define a spatial average $\langle\cdots\rangle$ of an observable $f(t,\boldsymbol{x})$ at time t as

$$\langle f\rangle_{\mathcal{D}(t)} = \frac{1}{V(t)}\int_{\mathcal{D}(t)} d^3x f(t,\boldsymbol{x}), \tag{2.11}$$

where $\mathcal{D}(t)$ is a spatial domain at time t and $V(t)$ is its volume defined by $V(t) = \int_{\mathcal{D}(t)} d^3x$. The observable $f(t,\boldsymbol{x})$ can be any function of $\theta, \rho, \sigma_\pm, E_\pm$. We would like to derive the expression for the infinitesimal scale change of the averaged observable on the same time slice, i.e.,

$$\frac{\Delta\langle f\rangle_{\mathcal{D}(t)}}{\Delta l} = \frac{\langle f\rangle_{\mathcal{D}'(t)} - \langle f\rangle_{\mathcal{D}(t)}}{\Delta l}, \tag{2.12}$$

where the parameter l measures the true scale change on this time slice, which is defined by

$$e^{\Delta l} \equiv e^{l'-l} = \left(\frac{V'(t)}{V(t)}\right)^{1/3}, \tag{2.13}$$

and is different from the naive scaling parameter τ. $\mathcal{D}'(t)$ and $V'(t)$ denote the domain and volume transformed back

to the original time t slice by time evolution from $\mathcal{D}'(t')$ and $V'(t')$, which are obtained by a scale transformation (2.10). The above Eq. (2.12) can be decomposed into two parts: (i) a change $\Delta_S\langle f\rangle$ associated with a scale transformation from $\mathcal{D}(t)$ to $\mathcal{D}'(t')$, (ii) a change $\Delta_T\langle f\rangle$ associated with a time evolution from $\mathcal{D}'(t')$ to $\mathcal{D}'(t)$. That is,

$$\frac{\Delta\langle f\rangle_{\mathcal{D}(t)}}{\Delta l}=\frac{1}{\Delta l}[(\langle f\rangle_{\mathcal{D}'(t')}-\langle f\rangle_{\mathcal{D}(t)})+(\langle f\rangle_{\mathcal{D}'(t)}-\langle f\rangle_{\mathcal{D}'(t')})]$$
$$\equiv\frac{1}{\Delta l}(\Delta_S\langle f\rangle+\Delta_T\langle f\rangle). \tag{2.14}$$

As for part (i), we use the scaling law of the observable $\langle f\rangle_{\mathcal{D}(t)}$, which is

$$\langle f\rangle_{\mathcal{D}(t)}\to\langle f\rangle_{\mathcal{D}'(t')}=e^{\alpha s\Delta\tau}\langle f\rangle_{\mathcal{D}(t)}. \tag{2.15}$$

The second part (ii) is given by the Taylor expansion of $f(t',\boldsymbol{x}')$ and $\mathcal{D}'(t')$ with respect to time:

$$\langle f\rangle_{\mathcal{D}'(t')}=\frac{1}{(1+\langle\theta\rangle_{\mathcal{D}'(t)}\Delta t)V'(t)}\int_{\mathcal{D}'(t')}\times(1+\theta\Delta t)d^3x'\left[f(t,\boldsymbol{x}')+\frac{df}{dt}(t,\boldsymbol{x}')\Delta t\right]$$
$$+O[(\Delta t)^2]=\langle f\rangle_{\mathcal{D}'(t)}+\Delta t\times\left(-\langle\theta\rangle_{\mathcal{D}'(t)}\langle f\rangle_{\mathcal{D}'(t)}+\langle\theta f\rangle_{\mathcal{D}'(t)}+\left\langle\frac{df}{dt}\right\rangle_{\mathcal{D}'(t)}\right)$$
$$+O[(\Delta t)^2], \tag{2.16}$$

where $\Delta t=t'-t$.

The true scale change Δl on a constant time slice is given as follows. In the scale transformation (i), the volume change is $V'(t')/V(t)=e^{3\Delta\tau}=1+3\Delta\tau$, but it includes the expansion effect of the Universe because time is also transformed. To obtain the true scale change on the same time slice, we have to transform it back to the original time slice by the time evolution (ii), which gives $V'(t')/V'(t)=1+\langle\theta\rangle\Delta t$. Then we have

$$\left(\frac{V'(t)}{V(t)}\right)^{1/3}=1+\Delta\tau-\frac{\langle\theta\rangle}{3}\Delta t=1+\Delta l. \tag{2.17}$$

Thus we obtain

$$\Delta l=\Delta\tau-\frac{\langle\theta\rangle}{3}\Delta t. \tag{2.18}$$

The time interval $\Delta t=t'-t$ is given by the scale transformation (2.10) as

$$\frac{\Delta t}{\Delta\tau}=st. \tag{2.19}$$

Hereafter we identify this fixed time t as the present cosmic time t_0, when we observe cosmological quantities.

Thus, combining Eqs. (2.14)–(2.19), we obtain the differential equation for the averaged observable $\langle f\rangle_{\mathcal{D}(t)}$:

$$\frac{d\langle f\rangle_{\mathcal{D}(t)}}{dl}=\mathcal{S}\left(\frac{\alpha}{t_0}\langle f\rangle_{\mathcal{D}(t)}+\langle\theta\rangle_{\mathcal{D}(t)}\langle f\rangle_{\mathcal{D}(t)}-\langle\theta f\rangle_{\mathcal{D}(t)}-\left\langle\frac{df}{dt}\right\rangle_{\mathcal{D}(t)}\right), \tag{2.20}$$

where

$$\mathcal{S}=\frac{s}{1-s\langle\theta\rangle_{\mathcal{D}(t)}t_0/3}. \tag{2.21}$$

The parameter s dependence appears solely through this factor $\mathcal{S}$.

Equation (2.20) is not yet sufficient to obtain a closed set of RG equations because of the nonlinearity of the basic equations. Differential equations for the nth order averaged quantities are not closed up to the nth order. They necessarily contain $(n+1)$th order averaged quantities. This is the famous Bogoliubov-Born-Green-Kirkwood-Yvon (BBGKY) hierarchy in statistical physics. The ordinary method to obtain the closed set of equations is to truncate this hierarchy at some order. In our case, we include the effect of fluctuations at the lowest nontrivial level, i.e., the second order cumulants. Then we will neglect all intrinsic fluctuations (cumulants) higher than the second order, finding the following truncation formula:

$$\langle fgh\rangle\to\langle f\rangle\langle gh\rangle+\langle g\rangle\langle fh\rangle+\langle h\rangle\langle fg\rangle-2\langle f\rangle\langle g\rangle\langle h\rangle. \tag{2.22}$$

To write down the basic equations, we shall use the second order cumulant $\langle fg\rangle_c$ instead of the averaged quadratic quantity $\langle fg\rangle$, where $\langle fg\rangle_c\equiv\langle fg\rangle-\langle f\rangle\langle g\rangle$. Applying this reduction, we obtain a closed set of 27 differential equations for averaged variables and their second order cumulants. We will present the complete expression in the Appendix. Here we only show a reduced set of equations to the first order (the averaged variables) by setting $\langle fg\rangle_c=0$:

$$\frac{d\langle\rho\rangle}{dl}=\mathcal{S}[\langle\theta\rangle-2]\langle\rho\rangle, \tag{2.23}$$

$$\frac{d\langle\theta\rangle}{dl}=\mathcal{S}\left[\left(\frac{\langle\theta\rangle}{3}-1\right)\langle\theta\rangle+4\pi G\langle\rho\rangle+6(\langle\sigma_+\rangle^2+\langle\sigma_-\rangle^2)\right], \tag{2.24}$$

$$\frac{d\langle\sigma_+\rangle}{dl}=\mathcal{S}\left[\left(\frac{2}{3}\langle\theta\rangle-1\right)\langle\sigma_+\rangle-\langle\sigma_+\rangle^2+\langle\sigma_-\rangle^2+\langle E_+\rangle\right], \tag{2.25}$$

$$\frac{d\langle\sigma_-\rangle}{dl}=\mathcal{S}\left[\left(\frac{2}{3}\langle\theta\rangle-1\right)\langle\sigma_-\rangle+2\langle\sigma_+\rangle\langle\sigma_-\rangle+\langle E_-\rangle\right], \tag{2.26}$$

$$\frac{d\langle E_+\rangle}{dl}=\mathcal{S}[(\langle\theta\rangle-2)\langle E_+\rangle+4\pi G\langle\rho\rangle\langle\sigma_+\rangle], \quad (2.27)$$

$$\frac{d\langle E_-\rangle}{dl}=\mathcal{S}[(\langle\theta\rangle-2)\langle E_-\rangle+4\pi G\langle\rho\rangle\langle\sigma_-\rangle]. \quad (2.28)$$

These also form a closed set of equations at this order. We call these first order RG equations, while those in the Appendix we call second order RG equations.

Here and in the Appendix, we have set $t_0=1$ and dropped the suffix of integration domain for averaged values just for simplicity. Hence, in these units, the expansion θ and the density ρ for Einstein–de Sitter universe turn out to be $\theta_{\rm EdS}=2$ and $\rho_{\rm EdS}=1/6\pi G$.

III. ANALYSIS OF RG EQUATIONS: FIXED POINTS AND RG FLOW

We now examine the RG equations obtained in Sec. II. First, we analyze the first order RG equations (2.23)–(2.28). Although this may not be realistic because the structure of the Universe could be highly inhomogeneous in our model, it shows that it is naive to understand the RG flow and give three important fixed points (including the Einstein–de Sitter spacetime), which will be also most relevant even in the case with fluctuations. We then examine the stability of these fixed points [18]. Next, introducing fluctuations, we study the second order RG equations (A1)–(A27) and analyze the stability of those fixed points in a much wider parameter space. Finally in this section, we set the Einstein–de Sitter fixed point with a small amount of fluctuation, as the boundary condition at the horizon scale in our present Universe and examine a scale dependence of averaged variables toward smaller scale.

A. Fixed points of the RG equations and stability

First we analyze the structure of our RG equations. From Eqs. (A1)–(A27), we find that they are written in a vector form as

$$\frac{d\langle F\rangle}{dl}=\mathcal{S}(A[\langle F\rangle]+C\langle FF\rangle_c) \quad (3.1)$$

$$\frac{d\langle FF\rangle_c}{dl}=\mathcal{S}B[\langle F\rangle]\langle FF\rangle_c, \quad (3.2)$$

where $\langle F\rangle$ and $\langle FF\rangle_c$ are 6- and 21-dimensional vectors defined as $\langle F\rangle\equiv(\langle f_i\rangle)$ and $\langle FF\rangle_c\equiv(\langle f_i f_j\rangle_c)$ with f_i's ($i=1\sim6$) denoting ρ, θ, σ_+, σ_-, E_+, and E_-. $A[\langle F\rangle]$, $B[\langle F\rangle]$, and C are six-dimensional vectors of quadratic functions of $\langle f_i\rangle$, 21×21 matrix of linear functions of $\langle f_i\rangle$, and 6×21 constant matrix, respectively. Setting $\langle FF\rangle_c=0$, we have

$$\frac{d\langle F\rangle}{dl}=\mathcal{S}A[\langle F\rangle], \quad (3.3)$$

which is exactly the first order RG equations (2.23)–(2.28).

To analyze the structure of the RG equations, we first need to know the fixed point $(\langle F\rangle,\langle FF\rangle)=(\langle F\rangle^*,\langle FF\rangle_c^*)$, which is defined by

$$\left.\frac{d\langle F\rangle}{dl}\right|_{\langle F\rangle=\langle F\rangle^*,\langle FF\rangle_c=\langle FF\rangle_c^*}=\left.\frac{d\langle FF\rangle_c}{dl}\right|_{\langle F\rangle=\langle F\rangle^*,\langle FF\rangle_c=\langle FF\rangle_c^*}=0. \quad (3.4)$$

As for the first order RG equations, the fixed point $\langle F\rangle=\langle F\rangle^*$ is given by

$$A[\langle F\rangle^*]=0. \quad (3.5)$$

The above Eqs. (3.1), (3.2), with (3.5) guarantee that the fixed points $\langle F\rangle^*$ in the first order RG equations are always those for the second order RG equations with $\langle FF\rangle_c^*=0$, although new additional fixed points appear in second order.

The stability analysis is very important to know asymptotic behaviors near the fixed points. The stability is examined by linearizing the RG equations around the fixed point $\langle F\rangle^*$, $\langle FF\rangle_c^*$ as

$$\langle F\rangle=\langle F\rangle^*+\mathcal{F}, \quad (3.6)$$

$$\langle FF\rangle_c=\langle FF\rangle_c^*+(\mathcal{FF})_c, \quad (3.7)$$

where both $\mathcal{F}$ and $(\mathcal{FF})_c$ are small enough to make the linear perturbation treatment effective around $\langle F\rangle^*$, $\langle FF\rangle_c^*$. Then, we find the perturbation equations in the form

$$\frac{d}{dl}\begin{pmatrix}\mathcal{F}\\(\mathcal{FF})_c\end{pmatrix}=\begin{pmatrix}\mathcal{W}_{11}&\mathcal{W}_{12}\\\mathcal{W}_{21}&\mathcal{W}_{22}\end{pmatrix}\begin{pmatrix}\mathcal{F}\\(\mathcal{FF})_c\end{pmatrix}, \quad (3.8)$$

where the perturbation matrix $\mathcal{W}^{[2]}=(\mathcal{W}_{AB})$ is given as

$$\begin{pmatrix}\mathcal{W}_{11}&\mathcal{W}_{12}\\\mathcal{W}_{21}&\mathcal{W}_{22}\end{pmatrix}=\begin{pmatrix}\left.\frac{\partial(\mathcal{S}A[\langle F\rangle])}{\partial\langle F\rangle}\right|_{\langle F\rangle=\langle F\rangle^*}&\mathcal{S}^*C\\\left.\frac{\partial(\mathcal{S}B[\langle F\rangle])}{\partial\langle F\rangle}\right|_{\langle F\rangle=\langle F\rangle^*}\langle FF\rangle_c^*&\mathcal{S}^*B[\langle F\rangle^*]\end{pmatrix}, \quad (3.9)$$

with $\mathcal{S}^*=\mathcal{S}|_{\langle F\rangle=\langle F\rangle^*}$. For the first order RG equations, it turns out to be

$$\frac{d\mathcal{F}}{dl}=\mathcal{W}^{[1]}, \quad (3.10)$$

where $\mathcal{W}^{[1]}$ is given as

$$\mathcal{W}^{[1]}=\mathcal{S}^*\left.\frac{\partial A[\langle F\rangle]}{\partial\langle F\rangle}\right|_{\langle F\rangle=\langle F\rangle^*}, \quad (3.11)$$

because of Eq. (3.5). For the fixed points in the first order RG equations, we find the following important results. As we

mentioned, they are also the fixed points in the second order with $\langle FF\rangle_c^*=0$. Then the perturbation matrix $\mathcal{W}^{[2]}$ becomes

$$\mathcal{W}^{[2]}=\begin{pmatrix} \mathcal{W}^{[1]} & \mathcal{S}^*C \\ 0 & \mathcal{S}^*B[\langle F\rangle^*] \end{pmatrix}. \tag{3.12}$$

This form guarantees that the eigenvalues of the first order matrix $\mathcal{W}^{[1]}$ are always those of the second order matrix $\mathcal{W}^{[2]}$. As we will show later, the other eigenvalues of the second order matrix are constructed by a sum of any two eigenvalues of the first order matrix [see Eqs. (3.20), (3.23)].

The positive (negative) eigenvalue of the matrix $\mathcal{W}^{[2]}$ (or $\mathcal{W}^{[1]}$) shows the instability (stability) of the fixed point $(\langle F\rangle^*,\langle FF\rangle_c^*)$ (or $\langle F\rangle^*$) toward the larger scale, i.e., in the large l direction. The stability and the instability are exchanged if we follow the RG flow in the opposite direction, i.e., toward the smaller scale.

The eigenvalues fully characterize the scale dependence of all physical variables in the vicinity of each fixed point. Although each observable is scaled according to its dimension, the effect of dynamics changes the scaling property from the original bare scaling law (2.10), so that the scaling of each observable is determined by the superposition of several eigenfunctions as follows:

$$\langle f_i\rangle=\langle f_i\rangle_*+\sum_{m=1}^{N}\epsilon_{i,m}e^{\lambda_m l}$$

$$\lambda_{\min}=\lambda_1\leqslant\lambda_2\leqslant\cdots\leqslant\lambda_N=\lambda_{\max}, \tag{3.13}$$

where $\langle f_i\rangle_*$ is the value of $\langle f_i\rangle$ at a fixed point, $\epsilon_{i,m}$ is some small constant, and λ_m $(m=1\sim N)$ are eigenvalues. $N=n(n+3)/2$ for the second order RG equations, while $N=n$ for the first order RG equations, with n being the number of observables. Since the maximum (minimum) eigenvalue $\lambda_{\max}(\lambda_{\min})$ becomes the most relevant toward larger (smaller) scale, the scaling property of each observable around fixed point is determined by $\lambda_{\max}(\lambda_{\min})$.

The fixed points themselves are independent of the scaling parameter s, but the matrix $\mathcal{W}^{[2]}$ (or $\mathcal{W}^{[1]}$) and its eigenvalues depend on s. For the sake of the explicit argument below, we restrict the range of the parameter s to $0<s<1$ where the topology of the RG flow is not changed [19].

B. Fixed points and the flow of RG equations without fluctuations

Here we analyze the first order RG equations (2.23)–(2.28) in detail. First, by neglecting both shear and tidal force terms, we have simple RG equations (3.3) with

$$A[\langle F\rangle]=\begin{pmatrix} -\langle\theta\rangle+\frac{1}{3}\langle\theta\rangle^2+4\pi G\langle\rho\rangle \\ (\langle\theta\rangle-2)\langle\rho\rangle \end{pmatrix} \tag{3.14}$$

for two averaged variables $\langle F\rangle=(\langle\rho\rangle,\langle\theta\rangle)$. We easily find three fixed points $\langle F\rangle_{(k)}^*$ $(k=1,2,3)$, which are listed in Table I.

The stability at each fixed point $\langle F\rangle_{(k)}^*$ is examined by linearizing the RG equations around the fixed point [Eq. (3.10)]. All eigenvalues of $\mathcal{W}^{[1]}$ for three fixed points are also given in Table I. For the first fixed point (1) where both $\langle\theta\rangle_{(1)}^*$ and $\langle\rho\rangle_{(1)}^*$ vanish, the dynamical term $\Delta_T\langle F\rangle$ does not affect the scaling, so that the eigenvector points the direction of each observable. On the other hand, for other fixed points, the effect of dynamics changes a scaling property from the original bare scaling law (2.10).

TABLE I. The list of three fixed points and their eigenvalues in the case with neither shear and tidal force nor fluctuations.

	$6\pi G\langle\rho\rangle^*$	$\langle\theta\rangle^*$	$\mathcal{S}^*$	Two eigenvalues
(1) Q	0	0	s	$\{-2\mathcal{S}^*,-\mathcal{S}^*\}$
(2) E	1	2	$\frac{3s}{3-2s}$	$\{-\frac{2}{3}\mathcal{S}^*,\mathcal{S}^*\}$
(3) M	0	3	$\frac{s}{1-s}$	$\{\mathcal{S}^*,\mathcal{S}^*\}$

As seen from Table I, the fixed point (1) is stable toward larger scale. For increasing scale, the Universe approaches this fixed point, at which both the energy density and expansion vanish. Therefore we shall call it the fixed point Q as the Universe is quiescent. The second fixed point (2) is a saddle point. It represents the Einstein–de Sitter Universe because $\langle\theta\rangle_{(2)}^*=\theta_{\rm EdS}$ and $\langle\rho\rangle_{(2)}^*=\rho_{\rm EdS}$. We thus call it the fixed point E. The third fixed point (3) is unstable in any direction. At first sight, it might look strange since the expansion of the Universe is finite in spite of vanishing energy density. This corresponds to the ''Milne'' universe in which the expansion rate is apparently finite because of a specific choice of the time slice. We call it the fixed point M. This Universe is reduced to the ''Minkowski'' space by adjusting the time slice appropriately.

In Fig. 1, to see more precisely those fixed points and the behaviors of global structure of the RG equations, we depict the RG flow on the H-Ω plane, where the Hubble parameter H and the density parameter Ω are defined by

$$H\equiv\frac{\langle\theta\rangle}{3}, \tag{3.15}$$

$$\Omega\equiv\frac{8\pi G\langle\rho\rangle}{3H^2}. \tag{3.16}$$

The RG flow either approaches fixed point Q or escapes to infinity toward larger scale. These two kinds of flows are clearly separated by the divide which passes through two fixed points E and M (Fig. 1). The flow escaping to infinity seems unphysical since both H and Ω blow up to infinity at large scale.

Next we include shear and tidal force, which leads to Eqs.(2.23)–(2.28). The three fixed points Q, M, and E found in the case without shear and tidal force survive, and their stabilities also remain unchanged (see Table II). In this sense, the three fixed points Q, M, and E are robust. Four new fixed points appear in addition to those three fixed

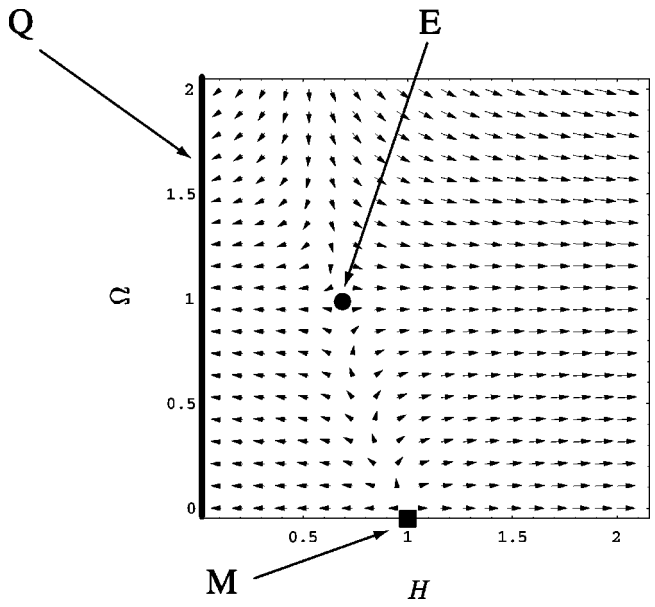

FIG. 1. The RG flow toward larger scale on the H-Ω plane in the case with neither shear nor fluctuations. Here we define the Hubble parameter H and the density parameter Ω as $H \equiv \langle \theta \rangle /3$ and $\Omega \equiv 8\pi G \langle \rho \rangle /3H^2$, respectively. The three important fixed points exist: (1) fixed point Q (quiescent Universe), (2) fixed point E (Einstein–de Sitter Universe), (3) fixed point M (Milne Universe). The RG flow converges to the fixed point Q or escapes to infinity. The fixed point seems to be a line in the H-Ω plane, but it is a point that all physical variables vanish in the ''phase'' space of $\langle F \rangle = (\langle \rho \rangle, \langle \theta \rangle)$. Ω turns out to be some finite value, which depends on the limit of $\langle \rho \rangle \to 0$ and $\langle \theta \rangle \to 0$.

points, which are listed in Table II. Since all new fixed points are saddle points, any RG flow still approaches the fixed point Q or escapes to infinity toward larger scale, or it approaches the fixed point M toward smaller scale.

C. Fixed points and the flow and of RG equations with fluctuations

Since our model of the Universe may be quite inhomogeneous and could be fractal in a microscopic point of view, an inclusion of fluctuations of the physical variables is inevitably important when we compare our results with those for the real Universe. In fact, if we do not include fluctuations, it is mathematically equivalent to a self-similar solution on a fixed time slice [20–22] although the physical meaning is quite different. Then, we shall add fluctuations and see how the fluctuations affect the RG flow diagram. We just include second order cumulants to the RG equations and truncate this hierarchy there by ignoring all intrinsic fluctuations (cumulants) higher than the second order, although we may have another choice of higher-order cumulants [23].

There are 27 independent variables in this case and it becomes more difficult to find a full list of fixed points. Thus we first reduce the number of variables and start our study from the shear-free case. Since independent observables are just ρ and θ in this case, the total number of variables including second order cumulants is just 5: $\langle \rho \rangle$, $\langle \theta \rangle$, $\langle \rho^2 \rangle_c$, $\langle \theta^2 \rangle_c$, $\langle \rho \theta \rangle_c$. We list all fixed points and show their stabilities in Table III. The three important fixed points (1)–(3) in the first order RG equations still remain and their stabilities are also unchanged. They are quite robust. Since all of the new fixed points (8)–(10) are saddle points, global properties of RG flows toward both larger and smaller scales are solely determined by the fixed points Q and M, respectively. The fixed point E remains as a saddle point.

As we mentioned, the fixed points found in the first order equations are also those of second order with zero cumulants. For the eigenvalues at those fixed points, we find eigenvalues of first order are also those of second order. To see more detail, we explicitly write down the perturbation matrix $\mathcal{W}^{[2]}$ (3.12) as

TABLE II. The list of seven fixed points and their eigenvalues in the case without fluctuations in LTA. The seventh fixed point (7) is not an isolated point but a closed loop parametrized by one parameter η as $\sigma_+^* = \frac{1}{3}\cos\eta$, $\sigma_-^* = \frac{1}{3}\sin\eta$, $E_+^* = \frac{1}{9}(\cos 2\eta - 3\cos\eta)$, $E_-^* = -\frac{1}{9}(\sin 2\eta + 3\sin\eta)$, where $0 \leqslant \eta < 2\pi$. $\bar{\lambda}_1, \bar{\lambda}_2, \bar{\lambda}_3$ are three real solutions ($-1 \leqslant \bar{\lambda}_1 < \bar{\lambda}_2 \leqslant 0$, $\bar{\lambda}_3 \geqslant 1$) of $\bar{\lambda}^3 - \bar{\lambda} - 4(1-\cos 3\eta)/27 = 0$.

	$6\pi G\langle\rho\rangle^*$	$\langle\theta\rangle^*$	$\langle\sigma_+\rangle^*$	$\langle\sigma_-\rangle^*$	$\langle E_+\rangle^*$	$\langle E_-\rangle^*$	$\mathcal{S}^*$	Six eigenvalues
Q	0	0	0	0	0	0	s	$\{-2\mathcal{S}^*, -2\mathcal{S}^*, -2\mathcal{S}^*, -\mathcal{S}^*, -\mathcal{S}^*, -\mathcal{S}^*\}$
(2) E	1	2	0	0	0	0	$\frac{3s}{3-2s}$	$\{-\frac{2}{3}\mathcal{S}^*, -\frac{2}{3}\mathcal{S}^*, -\frac{2}{3}\mathcal{S}^*, \mathcal{S}^*, \mathcal{S}^*, \mathcal{S}^*\}$
(3) M	0	3	0	0	0	0	$\frac{s}{1-s}$	$\{\mathcal{S}^*, \mathcal{S}^*, \mathcal{S}^*, \mathcal{S}^*, \mathcal{S}^*, \mathcal{S}^*\}$
(4)	0	1	$-\frac{1}{3}$	0	0	0	$\frac{3s}{3-s}$	$\{-\mathcal{S}^*, -\mathcal{S}^*, -\mathcal{S}^*, -\mathcal{S}^*, -\mathcal{S}^*, \mathcal{S}^*\}$
(5)	0	1	$\frac{1}{6}$	$\frac{1}{2\sqrt{3}}$	0	0	$\frac{3s}{3-s}$	$\{-\mathcal{S}^*, -\mathcal{S}^*, -\mathcal{S}^*, -\mathcal{S}^*, -\mathcal{S}^*, \mathcal{S}^*\}$
(6)	0	1	$\frac{1}{6}$	$-\frac{1}{2\sqrt{3}}$	0	0	$\frac{3s}{3-s}$	$\{-\mathcal{S}^*, -\mathcal{S}^*, -\mathcal{S}^*, -\mathcal{S}^*, -\mathcal{S}^*, \mathcal{S}^*\}$
(7)	0	2	σ_+^*	σ_-^*	E_+^*	E_-^*	$\frac{3s}{3-2s}$	$\{\bar{\lambda}_1\mathcal{S}^*, \bar{\lambda}_2\mathcal{S}^*, 0, 0, \mathcal{S}^*, \bar{\lambda}_3\mathcal{S}^*\}$

TABLE III. The list of fixed points and their eigenvalues in the case without shear and tidal force including fluctuations. New fixed points (8)–(10) are unphysical because $\langle\rho^2\rangle_c^*$ and/or $\langle\theta^2\rangle_c^*$ are negative.

	$6\pi G\langle\rho\rangle^*$	$\langle\theta\rangle^*$	$36\pi^2G^2\langle\rho^2\rangle_c^*$	$\langle\theta^2\rangle_c^*$	$6\pi G\langle\rho\theta\rangle_c^*$	$\mathcal{S}^*$	Five eigenvalues
(1) Q	0	0	0	0	0	s	$\{-4\mathcal{S}^*,-3\mathcal{S}^*,-2\mathcal{S}^*,-\mathcal{S}^*\}$
(2) E	1	2	0	0	0	$\frac{3s}{3-2s}$	$\left\{-\frac{4}{3}\mathcal{S}^*,-\frac{2}{3}\mathcal{S}^*,\frac{1}{3}\mathcal{S}^*,\mathcal{S}^*,2\mathcal{S}^*\right\}$
(3) M	0	3	0	0	0	$\frac{s}{1-s}$	$\{\mathcal{S}^*,\mathcal{S}^*,2\mathcal{S}^*,2\mathcal{S}^*,2\mathcal{S}^*\}$
(8)	0	$\frac{3}{2}$	0	$-\frac{9}{8}$	0	$\frac{2s}{2-s}$	$\{-\mathcal{S}^*,-\mathcal{S}^*,-\frac{1}{2}\mathcal{S}^*,-\frac{1}{2}\mathcal{S}^*,\mathcal{S}^*\}$
(9)	0	$\frac{9}{5}$	0	$-\frac{27}{25}$	$\frac{81}{250}$	$\frac{5s}{5-3s}$	$\left\{-\frac{1+\sqrt{13}}{5}\mathcal{S}^*,-\frac{2}{5}\mathcal{S}^*,-\frac{1}{5}\mathcal{S}^*,\frac{-1+\sqrt{13}}{5}\mathcal{S}^*,\mathcal{S}^*\right\}$
(10)	0	2	$-\frac{1}{4}$	-1	$\frac{1}{2}$	$\frac{3s}{3-2s}$	$\left\{-\frac{1+\sqrt{17}}{6}\mathcal{S}^*,0,\frac{-1+\sqrt{17}}{6}\mathcal{S}^*,\frac{2}{3}\mathcal{S}^*,\mathcal{S}^*\right\}$

$$\mathcal{W}^{[1]}\equiv\begin{pmatrix} w_{11} & w_{12}\\ w_{21} & w_{22}\end{pmatrix}=\mathcal{S}^*\begin{pmatrix} \langle\theta\rangle^*-2 & \langle\rho\rangle^*\\ 4\pi G & \frac{2}{3}\langle\theta\rangle^*-1\end{pmatrix},$$

$$\mathcal{S}^*C=\mathcal{S}^*\begin{pmatrix} 0 & 0 & 0\\ 0 & -\frac{2}{3} & 0\end{pmatrix},$$

$$\mathcal{S}^*B[\langle F\rangle^*]$$

$$=\mathcal{S}^*\begin{pmatrix} 2(\langle\theta\rangle^*-2) & 0 & 2\langle\rho\rangle^*\\ 0 & 2\left(\frac{2}{3}\langle\theta\rangle^*-1\right) & 8\pi G\\ 4\pi G & \langle\rho\rangle^* & \frac{5}{3}\langle\theta\rangle^*-3\end{pmatrix}$$

$$=\begin{pmatrix} 2w_{11} & 0 & 2w_{12}\\ 0 & 2w_{22} & 2w_{21}\\ w_{21} & w_{12} & w_{11}+w_{22}\end{pmatrix}. \tag{3.17}$$

Then the eigenvalue equation for the second order perturbation matrix $\mathcal{W}^{[2]}$ is

$$(\lambda^2-\mathrm{tr}\,\mathcal{W}^{[1]}\lambda+\det\mathcal{W}^{[1]})(\lambda-\mathrm{tr}\,\mathcal{W}^{[1]})(\lambda^2-2\,\mathrm{tr}\,\mathcal{W}^{[1]}\lambda+4\,\det\mathcal{W}^{[1]})=0. \tag{3.18}$$

Since the eigenvalue equation for the first order matrix $\mathcal{W}^{[1]}$ is

$$\lambda^2-\mathrm{tr}\,\mathcal{W}^{[1]}\lambda+\det\mathcal{W}^{[1]}=0, \tag{3.19}$$

supposing that $\lambda_1^{[1]}$ and $\lambda_2^{[1]}$ are its two solutions, we find the solutions of Eq. (3.18), $\lambda_i^{[2]}$ $(i=1\sim5)$, to be

$$\lambda_1^{[2]}=\lambda_1^{[1]},\quad \lambda_2^{[2]}=\lambda_2^{[1]},$$

$$\lambda_3^{[2]}=2\lambda_1^{[1]},\quad \lambda_4^{[2]}=\mathrm{tr}\,\mathcal{W}^{[1]}=\lambda_1^{[1]}+\lambda_2^{[1]},$$

$$\lambda_5^{[2]}=2\lambda_2^{[1]}. \tag{3.20}$$

Therefore the minimum eigenvalues at fixed points of first order, in particular the fixed points Q, E, and M, are given by

$$\lambda_{\min}^{[2]}=2\lambda_{\min}^{[1]}, \tag{3.21}$$

if $\lambda_{\min}^{[1]}<0$ (this is the case for the fixed points Q and E), otherwise,

$$\lambda_{\min}^{[2]}=\lambda_{\min}^{[1]} \tag{3.22}$$

(this is the case for the fixed point M).

Finally, we study a full model with 27 RG equations for 6 independent variables including shear and tidal force and their second order cumulants. Though it is very difficult to find all fixed points, all seven fixed points in the first order RG equations (listed in Table II) remain fixed points, as we mentioned. As for their eigenvalues, we also find the same result as that in the case without shear and tidal force, that is, the eigenvalue in the second order RG equations $\{\lambda_m^{[2]}|m=1,\ldots,n(n+3)/2\}$ are constructed by those in the first order $\{\lambda_m^{[1]}|m=1,\ldots,n\}$ as

$$\lambda_m^{[2]}=\lambda_m^{[1]}\quad\text{for}\quad m=1,\ldots,n$$

$$\lambda_m^{[2]}=\lambda_l^{[1]}+\lambda_{l'}^{[1]}\quad\text{for}\quad m=n+1,\ldots,n(n+3)/2$$

$$\text{with}\quad l,l'=1,\ldots,n, \tag{3.23}$$

where n is the number of observables. This result is understood from some special relation between the perturbation matrices $\mathcal{W}^{[1]}$ and $\mathcal{S}^*B[\langle F\rangle^*]$ [24]:

$$\mathcal{S}^*B_{ij,kl}[\langle F\rangle^*]=\frac{1}{2}[\delta_{ik}w_{jl}+\delta_{il}w_{jk}+\delta_{jk}w_{il}+\delta_{jl}w_{ik}], \tag{3.24}$$

where i,j,k,l denote the observables $\rho,\theta,\sigma_\pm,E_\pm$.

In Table IV, we have only listed three important fixed points Q, E, and M with their stabilities. These three fixed

TABLE IV. Three important fixed points and their eigenvalues in the case with shear and tidal force in LTA as well as fluctuations.

	$6\pi G\langle\rho\rangle^*$	$\langle\theta\rangle^*$	$\langle\text{others}\rangle^*$	$\mathcal{S}^*$	27 eigenvalues
(1) Q	0	0	0	s	$\{(-4\mathcal{S}^*)\times 6,(-3\mathcal{S}^*)\times 9,(-2\mathcal{S}^*)\times 9,(-\mathcal{S}^*)\times 3\}$
(2) E	1	2	0	$\frac{3s}{3-2s}$	$\{(-\frac{4}{3}\mathcal{S}^*)\times 6,(-\frac{2}{3}\mathcal{S}^*)\times 3,(\frac{1}{3}\mathcal{S}^*)\times 9,$ $(\mathcal{S}^*)\times 3,(2\mathcal{S}^*)\times 6\}$
(3) M	0	3	0	$\frac{s}{1-s}$	$\{(\mathcal{S}^*)\times 6,(2\mathcal{S}^*)\times 21\}$

points still survive and their stabilities remain unchanged even after including fluctuations as well as shear and tidal forces.

Let us just mention how our results change if we use another approximation scheme for the equation of motion for E_{ij}. We mainly use the LTA approximation in this paper. In the case of other local approximations such as NMA [25], the RG equations become more complicated and it is more difficult to look for all fixed points and eigenvalues. However, it is still easy to show that the above three fixed points Q, M, and E survive since the RG equations exactly reduce to the shear-free case when we set $E_{\pm}=\sigma_{\pm}=0$. The stabilities of these fixed points can also be checked by examining the RG flow around them. We show that the stabilities of these fixed points remain unchanged even in the NMA. The minimum eigenvalue, which is the most relevant toward smaller scale, is also invariant irrespective of local approximation scheme of E_{ij}, because the eigendirection for $\lambda^{[2]}_{\rm min}$ (or $\lambda^{[1]}_{\rm min}$) is orthogonal to both shear and tidal directions in 27-dimensional ''phase'' space of $(\langle F\rangle,\langle FF\rangle_c)$ (or in six-dimensional ''phase'' space of $\langle F\rangle$). Hence the effect of shear or tidal force seems irrelevant to the scaling property of observables around fixed point E or M toward smaller scale.

The three fixed points E, M, and Q are robust and change neither their stability nor the scaling property of observables around them toward smaller scale, regardless of shear, tidal force, and the approximation scheme of the tidal force.

D. The flow of our Universe

The RG flow and the fixed points we argued in the previous subsections describe the diversity of our system. Only a part of them, i.e., a particular integral line in the flow diagram which satisfies a certain boundary condition, actually describes our real Universe. In order to elucidate such an integral flow, we need a plausible boundary condition and we need to examine the global and local scaling properties of the observables.

One plausible boundary condition at the present horizon scale and beyond could be the fixed point E (Einstein–de Sitter Universe). This boundary condition would be inferred from the inflationary scenario in the early Universe, which predicts the flat FRW Universe with tiny fluctuations similar to our real Universe.

With this boundary condition, we solve the RG equations toward smaller scale and study the scale change of various observables. In solving the RG equations toward the smaller scale, we must remember that (i) the positive (negative) eigenvalue of the matrix $\mathcal{W}^{[2]}$ at a fixed point denotes stability (instability). (ii) The direction of the integration is opposite to that of flow indicated in Fig. 1. It is clear that the choice of the exact values of point E as a boundary condition is trivial and not interesting because it is the fixed point and the flow stays there forever. To find more interesting model of the Universe, we need to start from the close vicinity of the fixed point E.

Here we choose the boundary condition as follows. For the averaged variables, we use the exact value of the fixed point E:

$$\langle\theta\rangle=\theta_{\rm EdS}=2,\quad \langle\rho\rangle=\rho_{\rm EdS}=1/6\pi G,\quad \langle\sigma_{\pm}\rangle=\langle E_{\pm}\rangle=0, \tag{3.25}$$

which gives $\Omega=1$. Since we expect some fluctuations even in an inflationary model, we set small finite fluctuations at the fixed E point. We assume that the off-diagonal fluctuations have initially no intrinsic fluctuations [26], i.e.,

$$\langle f_i f_j\rangle_c=0 (i\neq j)\ \ (\text{at}\ \ l=0). \tag{3.26}$$

Before going to show our numerical result, we shall discuss the asymptotic behaviors near three robust fixed points Q, E, and M. We showed that the scaling property of observables around those fixed points toward smaller scale is determined by the minimum eigenvalue $\lambda^{[2]}_{\rm min}$. This is always true for the second order cumulants $\langle f_i f_j\rangle_c$. The scaling property of the averaged variable $\langle f_i\rangle$ may, however, depend on the case, because the eigenvector with the eigenvalue $\lambda^{[1]}_{\rm min}$ is perpendicular to the hypersurface of the cumulants in the ''phase'' space $(\langle F\rangle,\langle FF\rangle_c)$. If we have fluctuations initially rather than a deviation from the fixed point, i.e., $\langle f_i^2\rangle_c^*\neq 0$, then

$$\langle f_i\rangle\sim\langle f_i\rangle^*+\epsilon_i e^{\lambda^{[2]}_{\rm min} l}, \tag{3.27}$$

as l decreases, unless $\langle f_i^2\rangle_c^*\gtrsim(\langle f_i\rangle^*)^2$. This is just because how to leave from the fixed point is determined by the fluctuations $\langle f_i^2\rangle_c^*$, which scaling property is fixed by $\lambda^{[2]}_{\rm min}$. On the other hand, if we have an initial deviation from the fixed point such as $\langle f_i\rangle\neq\langle f_i\rangle^*$ without the initial cumulant $(\langle f_i^2\rangle_c^*=0)$, then $\langle f_i\rangle-\langle f_i\rangle^*$ behaves first as $\exp(\lambda^{[1]}_{\rm min} l)$. Since our boundary condition is the former case, we expect an asymptotic behavior similar to Eq. (3.27).

It may be more comprehensive to show our results if we introduce the ''dispersions'' Δ_{ij} instead of the cumulants $\langle f_i f_j\rangle_c$. For the diagonal cumulants $\langle f_i^2\rangle_c$, we define them as

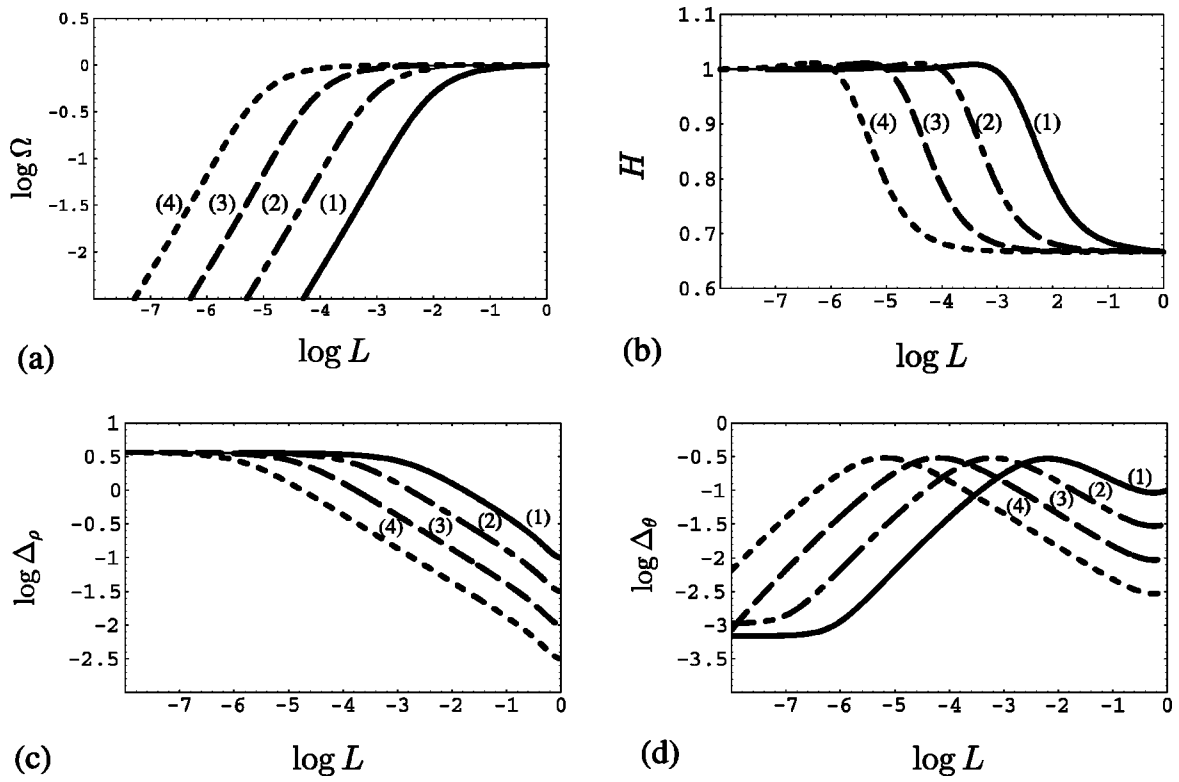

FIG. 2. The scale dependence of (a) $\ln\Omega$, (b) H, (c) Δ_ρ, and (d) Δ_θ in the shear-free case with $s=0.5$ and $\Delta_0=(1)10^{-1}$, $(2)10^{-1.5}$, $(3)10^{-2}$, $(4)10^{-2.5}$. We solve the RG flows from the fixed point E toward smaller scale. $L\equiv\exp l$ represents the ratio of the scale of averaged region to the horizon scale. Every flow monotonically converges to M as H becomes larger ($H\nearrow$) and Ω gets smaller ($\Omega\searrow$) toward smaller scale. The critical scale where Ω and H deviate from the EdS values depends on the magnitude of Δ_0.

$$\Delta_\rho^2=\langle\rho^2\rangle_c/\langle\rho\rangle^2,\quad \Delta_\theta^2=\langle\theta^2\rangle_c/\langle\theta\rangle^2,$$
$$\overline{\Delta}_{\sigma_\pm}^2=\langle\sigma_\pm^2\rangle_c/\langle\theta\rangle^2,\quad \overline{\Delta}_{E_\pm}^2=\langle E_\pm^2\rangle_c/\langle\theta\rangle^4, \qquad (3.28)$$

where for shear and tidal force, $\overline{\Delta}_{\sigma_\pm}$ and $\overline{\Delta}_{E_\pm}$, which are normalized by $\langle\theta\rangle$, have been used rather than the conventional dispersions because those averaged variables sometimes vanish even if their cumulants are finite, resulting in a divergence of the dispersions. The dispersion parameters $\Delta_\rho,\Delta_\theta,\overline{\Delta}_{\sigma\pm},\overline{\Delta}_{E\pm}$ are assumed to be sufficiently small at the boundary $l=0$. In what follows, just for simplicity, we also set $\Delta_\rho=\Delta_\theta\equiv\Delta_0$ at $l=0$, which may be plausible because ρ and θ may be closely connected with each other through the fluid equations and are expected to have the same order of fluctuations.

1. The case without shear and tidal force

First we consider the case without shear and tidal force. In Fig. 2, we depict the scale dependence of $\Omega,H,\Delta_\rho,\Delta_\theta$ in terms of $L\equiv e^l$, which is the ratio of the averaging scale to the horizon scale (or the scale at our boundary). Since we have chosen $l=0$ as the horizon scale (or beyond), our observable Universe is described by negative l. As seen from Fig. 2, the integrated flow line always converges to the values at fixed point M, i.e., $\Omega_{\rm Milne}=0$ and $H_{\rm Milne}=1$. This means that the Milne Universe is the unique stable fixed point toward smaller scale. Once it comes close to fixed point M, the behavior of the RG flow at small scale is determined by the minimum eigenvalue at M, i.e., $\lambda_{\rm min}^{[2]}=s/(1-s)$.

To see the role of the scaling parameter s, in Fig. 3 we plot the scale dependence of the density parameter Ω, the expansion H, and the fluctuations $\Delta_\rho,\Delta_\theta$ for several values of s with fixed initial fluctuations $\Delta_0=10^{-2}$. We find that the observables show the following universal behavior: (i) H increases toward smaller scale from 2/3 to 1; (ii) Ω reduces from 1 to 0 toward smaller scale. There is a plateau near the fixed point E, while a constant slope is found near the fixed point M.

The asymptotic values are given by those at the fixed points E and M. We can also explain the constant slope at the smaller scale and the plateau at the larger scale in the Ω diagram. Since $\langle\rho\rangle\sim O(\exp\{[s/(1-s)]l\})$ and $\langle\theta\rangle\sim 3$ near the fixed point M, Ω at smaller scale behaves as

$$\Omega\sim O(\exp\{[s/(1-s)]l\}), \qquad (3.29)$$

where $s/(1-s)$ is the minimum eigenvalue evaluated at the fixed point M. Then the slope of the Ω curve near M turns out to be

$$\frac{d\ln\Omega}{d\ln L}\sim\frac{s}{1-s}. \qquad (3.30)$$

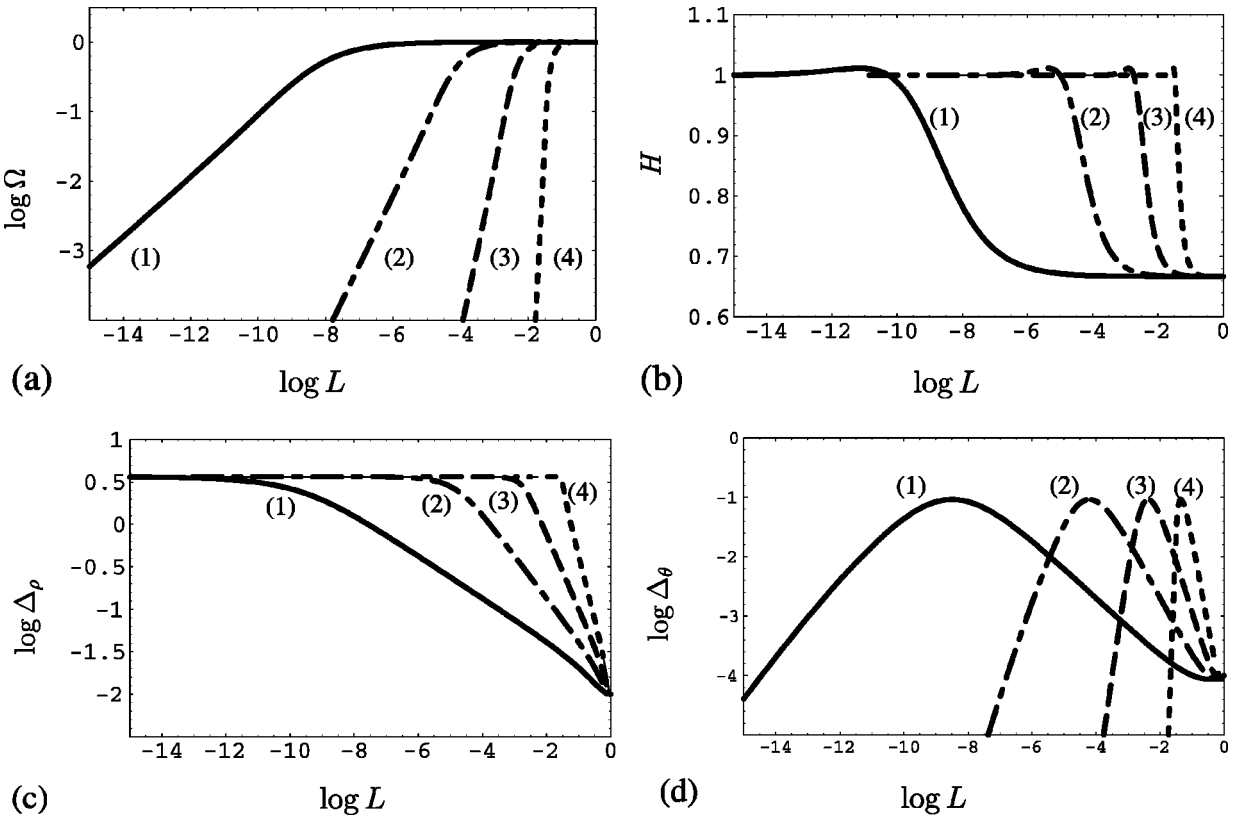

FIG. 3. The s dependence of the RG flows of (a) ln Ω, (b) H, (c) Δ_ρ, and (d) Δ_θ from the fixed point E at horizon scale in the shear-free case. Here we depict the cases of $\Delta_0=10^{-2}$ and $s=$(1) 0.3, (2) 0.5, (3) 0.7, (4) 0.9. Ω begins to decline beyond a critical scale, a few decades smaller than horizon scale, which depends on the magnitude of Δ_0. The slope at smaller scale is determined by $\lambda_{\min}^{[2]}=s/(1-s)$ at the fixed point M. The slope for the case (2) is equal to 1. H also changes from the value at E to the value at M beyond the above critical scale. As the value of s increases, the critical scale shifts toward smaller scale.

On the other hand, the plateau appears near the fixed point E, because

$$\langle\rho\rangle/\rho_{\rm EdS}\sim 1+\epsilon_\rho\exp\{-[2s/(3-2s)]l\},$$

$$\langle\theta\rangle/\theta_{\rm EdS}\sim 1+\epsilon_\theta\exp\{-[2s/(3-2s)]l\}, \qquad (3.31)$$

and then

$$\Omega\sim 1+(\epsilon_\rho-2\epsilon_\theta)\exp\{-[2s/(3-2s)]l\}\approx 1, \quad (3.32)$$

where we have used $\lambda_{\min}^{[2]}=-2s/(3-2s)$ evaluated at E. The turning point $L_{\rm cr}$ of the slope into the plateau is estimated easily, since the deviations from the EdS values are due to the fluctuations Δ_0, ϵ_ρ, $\epsilon_\theta\sim O(\Delta_0)$. Then, when $\Delta_0\exp\{-[2s/(3-2s)]l_{\rm cr}\}\sim O(1)$, i.e.,

$$\ln L_{\rm cr}=l_{\rm cr}\sim[(3-2s)/2s]\ln\Delta_0, \qquad (3.33)$$

we find a large deviation from the EdS values. Thus the minima of the eigenvalues at two fixed points E and M determine the asymptotic structure of our Universe.

Is there any observational data which may suggest a scale dependence of either Ω or density? In discussions of dark matter, when we plot the mass-luminosity ratio in terms of the scale of the objects, we find a curve similar to Fig. 3(a). If we assume that the mass-luminosity ratio curve is what we are discussing here, we find some constraint of s, such as $0.3\lesssim s\lesssim 0.7$.

2. The case with shear and tidal forces

Next, we examine the effect of shear and tidal forces. Just for simplicity we assume that $\sigma_-=E_-=0$, which is consistent with the RG equations. As we assumed, $\langle\sigma_+\rangle$ and $\langle E_+\rangle$ vanish at $l=0$. Then the initial free parameters are Δ_0, $\overline{\Delta}_{\sigma_-,0}$, and $\overline{\Delta}_{E_-,0}$, which are fluctuations at $l=0$. Our numerical calculations, shown in Figs. 4 and 5, reveal that they tend to prevent H and Ω from converging to the fixed point M though the Milne Universe is still a stable fixed point. More precisely, we observe three qualitatively different behaviors of the RG flow of our Universe.

(i) The RG flow monotonically converges to fixed point M. H and Ω approach the value determined by fixed point M toward a smaller scale.

(ii) Initially the Universe comes near the fixed M point, resulting in an increase of H and a decrease of Ω toward smaller scale. However, it turns around before reaching the

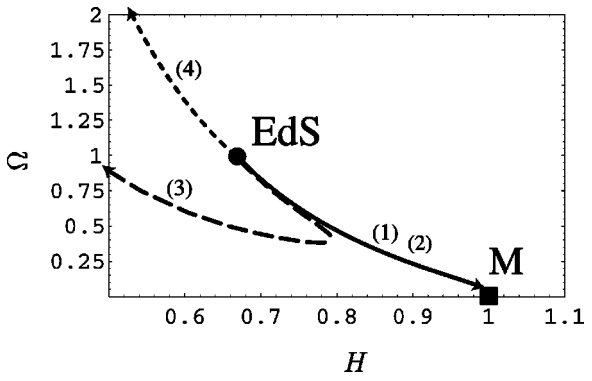

FIG. 4. The RG flow toward smaller scale on the H-Ω plane in the case that $s=0.5$ and $\bar{\Delta}_{\sigma_+,0}=\bar{\Delta}_{E_+,0}=10^{-2}$. As for the density perturbations, we choose $\Delta_0=$(1)$10^{-0.75}$, (2)10^{-1}, (3)$10^{-1.25}$, (4)$10^{-1.5}$. If both $\bar{\Delta}_{\sigma_+,0}/\Delta_0$ and $\bar{\Delta}_{E_+,0}/\Delta_0$ are less than $R_{\rm cr}\approx 0.1495$ [(1), (2)], every flow converges to M as H increases ($H\nearrow$) to 1 and Ω decreases ($\Omega\searrow$) to 0 toward smaller scales. On the other hand, if $\bar{\Delta}_{\sigma_+,0}$ or $\bar{\Delta}_{E_+,0}$ are larger than the above critical value $R_{\rm cr}$ [(3), (4)], the flow heading for M comes to turn around and go away to infinity.

fixed point M and eventually diverges to infinity in the flow diagram as $H\to-\infty$ and $\Omega\to\infty$.

(iii) The RG flow monotonically diverges to infinity in the flow diagram as $H\to-\infty$ and $\Omega\to\infty$.

We can classify the parameter space $(\Delta_0,\bar{\Delta}_{\sigma+,0},\bar{\Delta}_{E+,0})$ of fluctuations at the boundary (near the horizon) into three regions according to the above asymptotic behaviors of the RG flow. Class (i) is realized if the fluctuations of shear and tidal forces are sufficiently smaller than those of the density and the expansion, i.e., $\bar{\Delta}_{\sigma_+,0}/\Delta_0\sim\bar{\Delta}_{E_+,0}/\Delta_0<R_{\rm cr}$. Otherwise, i.e., if $\bar{\Delta}_{\sigma_+,0}/\Delta_0\sim\bar{\Delta}_{E_+,0}/\Delta_0>R_{\rm cr}$, class (iii) will happen. The critical value $R_{\rm cr}$ is almost independent of Δ_0 and approximately $R_{\rm cr}\approx 0.15$. Class (ii) is a narrow boundary between them. Hence, class (i) [or (ii)] naturally occurs as long as the shear and tidal force are sufficiently smaller than the density fluctuations at the horizon scale. This situation is strongly suggested by recent observations [27], i.e., the shear is strictly restricted to around $\sigma/H<10^{-9}$ by CMB data. Hence we expect that our Universe belongs to class (i) and its flow line converges into the fixed point M in smaller scale. The s dependence of Ω or H is quite similar to the case without shear and tidal forces [Figs. 6(a) and 6(b)].

As for the shear and tidal forces, their averaged values increase toward smaller scale, but eventually decrease if the flow converges to the fixed point M [Figs. 6(c) and 6(d)]. The scaling properties of the shear $\langle\sigma_+\rangle$ and the tidal force $\langle E_+\rangle$ are also determined by $\lambda^{[2]}_{\rm min}$ at the fixed points E and M. Both shear and tidal force are dumped off at smaller scale along the flow converging to the fixed point M.

The behaviors of fluctuations Δ_ρ, Δ_θ, $\bar{\Delta}_{\sigma_+}$, and $\bar{\Delta}_{E_+}$ are shown in Figs. 6(e)–6(h). We find similar behaviors to the case without shear and tidal forces for Δ_ρ and Δ_θ.

E. Beyond the horizon scale

In the previous subsections, we have integrated the RG equations from the horizon scale ($l=0$) toward the smaller scale. It is also possible to solve them toward the larger scale with the same boundary conditions. The structure beyond the horizon scale is not observable at present but may give some relation with an inflationary scenario in the early Universe. In Fig. 7, we plot the scale dependence of $\langle\rho\rangle$, H, and those fluctuations Δ_ρ and Δ_θ in the shear-free case with initial fluctuation $\Delta_0=10^{-2.5}$. In the finite scale $10^{-5}<L<10^5$, the flow stays in the vicinity of fixed point E and the power law behaviors of Δ_ρ and Δ_θ toward larger scale are determined by $\lambda^{[2]}_{\rm max}$ at fixed point E, while in larger scale $L>10^5$, the flow converges to fixed point Q after H becomes negative and their power law behaviors are characterized by the eigenvalues of $\mathcal{W}^{[2]}$ at the fixed point Q. These eigenvalues are the same ones naively determined from the original scaling. This is consistent with the fact that the expansion ceases at the fixed point Q and the RG transformation reduces to a pure scale transformation. This property makes Δ_ρ constant around fixed point Q because of the cancellation between numerator and denominator in the definition of Eq. (3.28) [Fig. 7(c)], while Δ_θ diverges at the scale where H vanishes and turns negative from the definition (3.28) [Fig. 7(d)]. The declination of the slope in the $\ln\langle\rho\rangle-\ln L$ diagram [Fig. 7(a)] is $-2s$ which is the minimum eigenvalue of $\mathcal{W}^{[2]}$ associated with the fixed point Q. If we assign a fractal dimension D for this Universe, $D=3-2s$ because $\langle\rho\rangle$ reduces as $e^{(D-3)l}$ from a fractal structure while $\langle\rho\rangle\propto e^{-2sl}$ by our scaling law. If we assign the value $s=0.5$, the corresponding fractal dimension becomes $D=2$. Because our model is a Newtonian cosmology, further analysis beyond the horizon scale would be irrelevant to the real Universe.

IV. CONCLUDING REMARKS

The renormalization group method has been applied to Newtonian cosmology in this paper and the scale dependence of the averaged observables on a fixed time slice including effects of fluctuations has been studied. The scaling assumption we proposed for the averaged observables is fulfilled in the case of either homogeneous distribution or nonanalytic distribution such as a fractal, if we assume such a scaling at any position and at fixed time. Actual observation of the two point correlation function of galaxies may favor such a fractality at least in the finite scale range below 10 Mpc. Multifractality could be applied to explain the transition from finite fractal range at smaller scale to homogeneous distribution at larger scale [28]. Our scaling analysis of averaged observables here might give a hint to the behavior of observables in such a fractal matter distribution, if it exists.

To close our dynamical system and apply the RG method, here we have adopted an approximation of tidal force (LTA) and considered only fluctuations up to second order. The higher order cumulants of averaged observables are ignored. We have found three robust fixed points of the RG equations: (1) The fixed point Q (quiescent Universe) is stable in any direction toward larger scale; (2) the fixed point E (Einstein–de Sitter Universe) is a saddle point; (3) the fixed point M (Milne Universe) is unstable in any direction toward larger scale.

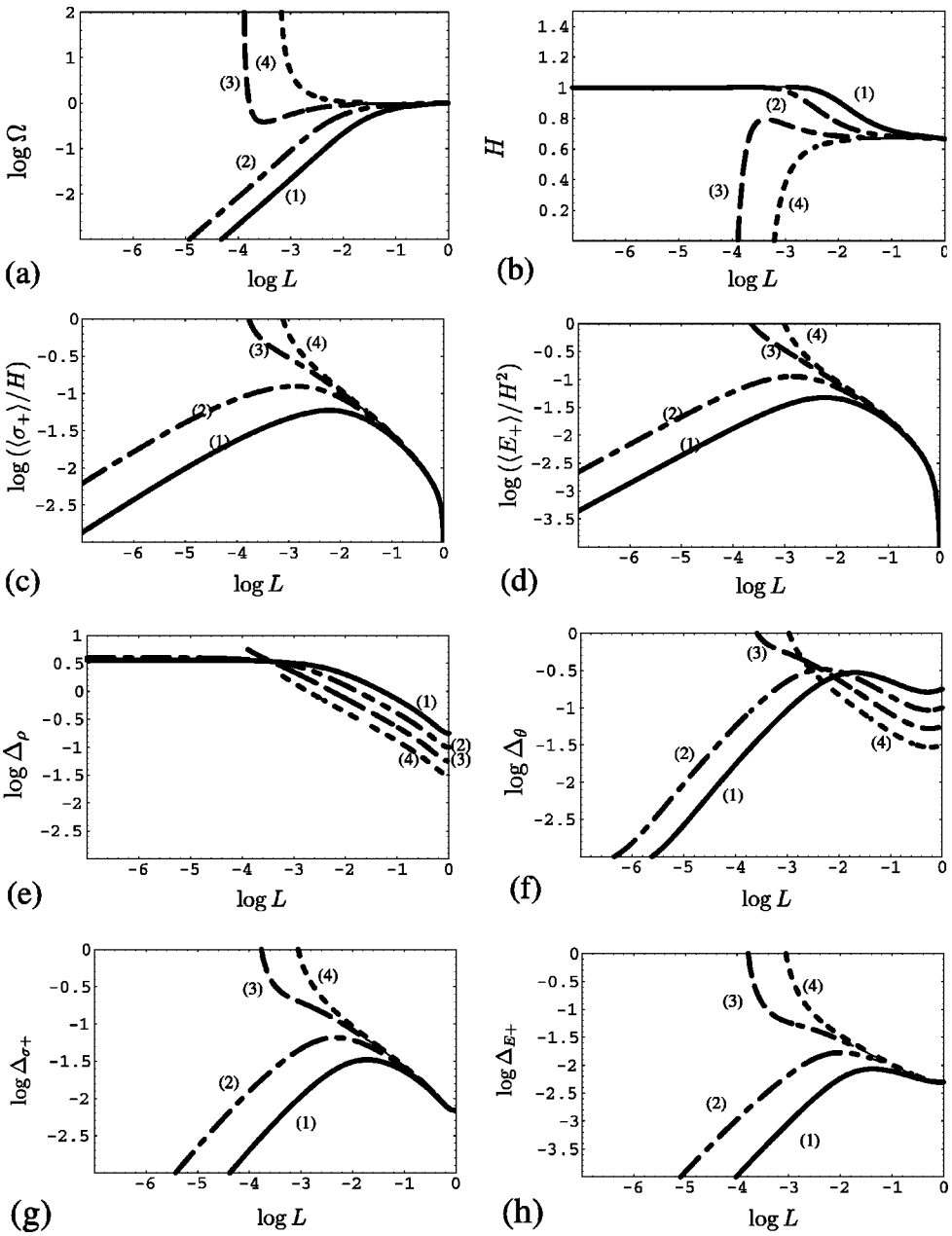

FIG. 5. The RG flow of (a) ln Ω, (b) H, (c) $\ln(\langle\sigma_{\pm}\rangle/H)$, and (d) $\ln(\langle E_{\pm}\rangle/H^2)$ from the fixed point E toward smaller scale in the case that $s=0.5$, $\bar{\Delta}_{\sigma_+,0}=\bar{\Delta}_{E_+,0}=10^{-2}$, and $\Delta_0=(1)10^{-0.75}$, $(2)10^{-1}$, $(3)10^{-1.25}$, $(4)10^{-1.5}$. In the case of (1) or (2) ($\bar{\Delta}_{\sigma_+,0}/\Delta_0, \bar{\Delta}_{E_+,0}/\Delta_0 \lesssim R_{\rm cr}\approx 0.1495$), the RG flow converges to M toward smaller scales as the case without shear and tidal force (see Fig. 2). In the case of (3) or (4) ($\bar{\Delta}_{\sigma_+,0}/\Delta_0, \bar{\Delta}_{E_+,0}/\Delta_0 \gtrsim R_{\rm cr}$), however, the RG flow does not converge to M but rather diverges to infinity. We also depicted the flow of fluctuations; (e) ln Δ_ρ, (f) ln Δ_θ, (g) ln $\bar{\Delta}\sigma_+$, and (h) ln $\bar{\Delta}_{E_+}$ for the same initial values as the above. In the case of (1) or (2), all fluctuations but Δ_ρ damp off as the RG flow converges to M, while Δ_ρ approaches the finite value. In the case of (3) or (4), all of them diverge to infinity.

These fixed points do not change their stability even if we extend the ''phase'' space including fluctuations as well as shear and tidal forces. Any other fixed points are saddle, and therefore the scaling property of the global RG flow toward larger (smaller) scale is determined by fixed point Q (M). We find that the Universe asymptotically approaches fixed point Q or diverges toward infinity regardless of the detail at the smaller scale.

In order to find out the flow line which represents our real Universe, we have imposed the boundary condition fixed point E with tiny fluctuations at the horizon scale. The inflationary scenario in the early Universe would imply such a boundary condition, i.e., the inflation predicts the Einstein–de Sitter Universe at the horizon scale and beyond. We have solved the RG equation toward smaller scale from this boundary. Then we find that, toward smaller scale, the

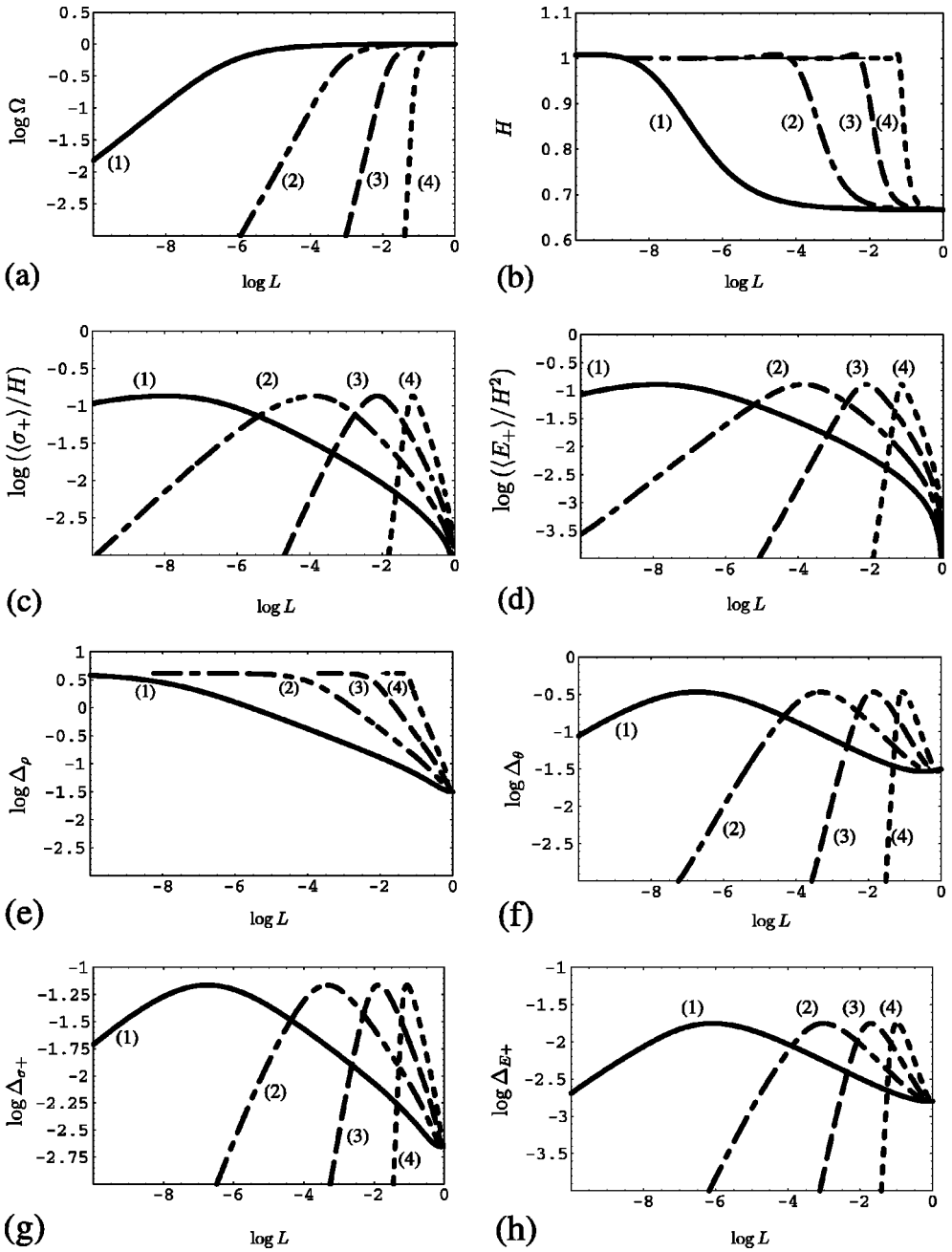

FIG. 6. The s dependence of the RG flows from fixed point E of (a) ln Ω, (b) H, (c) ln($\langle\sigma_{\pm}\rangle/H$), and (d) ln($\langle E_{\pm}\rangle/H^2$). Here we depict the cases of $s=(1)\,0.3,\ (2)\,0.5,\ (3)\,0.7,\ (4)\,0.9$ with the boundary conditions, $\Delta_0=10^{-1.5}$ and $\overline{\Delta}_{\sigma_+,0}=\overline{\Delta}_{E_+,0}=10^{-2.5}$ at horizon scale. The results for ln Ω and H are quite similar to Fig. 3, if the flow converges to the fixed point M. The slopes of $\langle\sigma_{\pm}\rangle$ and $\langle E_{\pm}\rangle$ at larger and smaller scale are determined by $\lambda^{[2]}_{\rm min}$ at fixed points E and M, i.e., $-4s/(3-2s)$ and $2s/(1-s)$, respectively. As s increases, the turning point of the slope shifts toward smaller scale and the slope becomes less steep. We also depicted the flow of fluctuations; (e) ln Δ_ρ, (f) ln Δ_θ, (g) ln $\overline{\Delta}_{\sigma_+}$, and (h) ln $\overline{\Delta}_{E_+}$ for the same range of s. $\Delta_0=10^{-1.5}$ and $\overline{\Delta}_{\sigma_+,0}=\overline{\Delta}_{E_+,0}=10^{-2.5}$ at horizon scale in the case of LTA. We find that $\Delta_\rho^2=$const near the fixed point M, while it decreases linearly near the fixed point E, which behavior is determined by the eigenvalue $-4s/(3-2s)$.

expansion H defined by $\langle\theta\rangle/3$ monotonically increases from 2/3 to 1, and the density parameter $\Omega=8\pi G\langle\rho\rangle/3H^2$ monotonically reduces from 1 to 0, provided the fluctuations of shear and tidal force are much smaller than the density fluctuations, which would be supported by the inflationary scenario [29] and observations of CMB.

We have two important free parameters, s and Δ_0. These values might be fixed by some of the following arguments: (i) The scale dependence of the mass-luminosity ratio of astrophysical objects; (ii) a systematic decrease of the Hubble

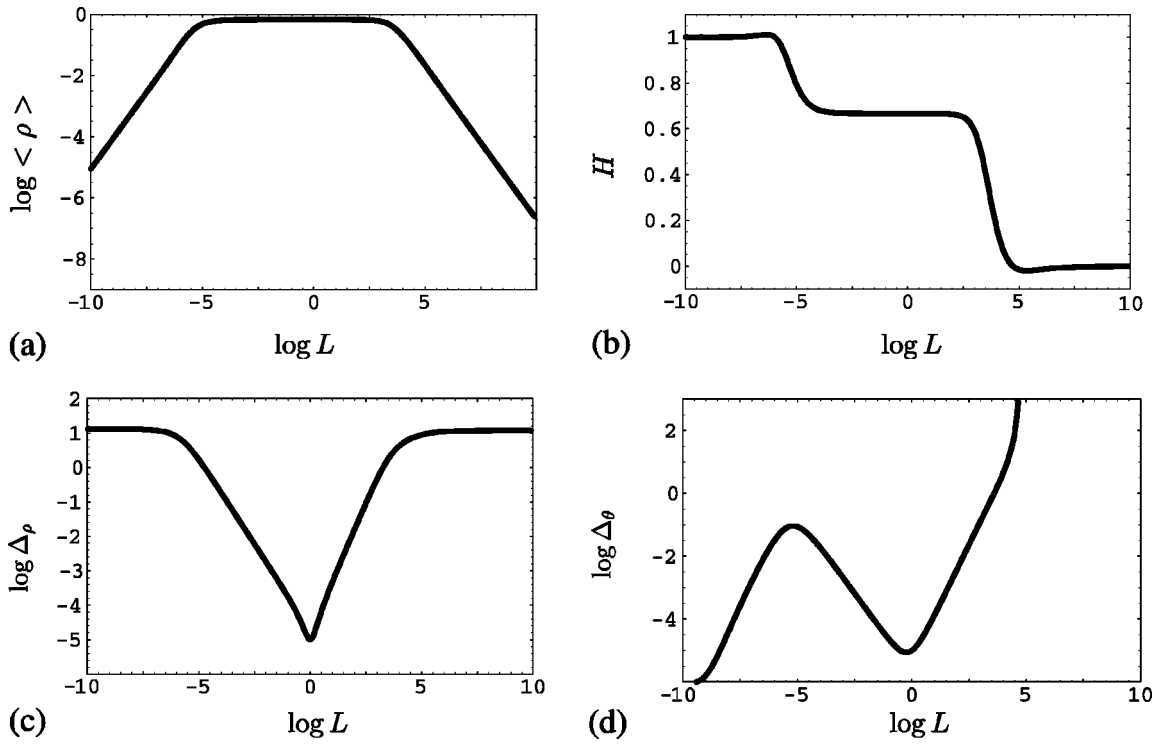

FIG. 7. The scale dependence of (a) $\ln\langle\rho\rangle$, (b) H, (c) $\ln\Delta_\theta$, and (d) $\ln\Delta_\rho$ beyond horizon scale for $s=0.5$ with the boundary conditions, $\Delta_0=10^{-2.5}$ at horizon scale in the shear-free case. In the flow departing from the fixed point E, $\langle\rho\rangle$ approaches zero toward both smaller and larger scales, for which the slopes at larger and smaller scale are determined by $\lambda^{[2]}_{\rm min}$ at fixed points, Q and M, i.e., $-2s$ and $2s/(1-2s)$, respectively. H also vanishes at larger scale, after it becomes negative around $L=10^5$, which causes the divergence of Δ_θ around the scale. The slope of both Δ_ρ and Δ_θ around the fixed point E are determined by $\lambda^{[2]}_{\rm min}=-4s/(3-2s)$ toward smaller scale and $\lambda^{[2]}_{\rm max}=6s/(3-2s)$ toward larger scale at the point.

parameter H, if any, toward the larger scale; (iii) the scale dependence of the amplitude of the two point correlation functions; (iv) some of the inflationary models predict a fractal-like structure beyond the horizon scale [30].

Several comments related with our future work are in order.

(a) We definitely need the general relativistic generalization of our work. This is because the large scale structures at high redshift and beyond the horizon scale would be adequately described only by general relativity.

(b) In our analysis, we assume a scaling property of the averaged observables and their fluctuations. However, we do not know whether such a solution is dynamically stable or not. To answer for this, we have to consider the dynamical stability of our system.

(c) So far we have considered fluctuations of variables up to second order. Though this would be sufficient when we consider the vicinity of the horizon scale, we ultimately need to incorporate higher order fluctuations as well for the consistency of the theory.

(d) We have used the local tidal approximation (LTA) for obtaining equations of motions for tidal force. By this method, we could avoid directly solving the Poisson equation. This approximation would be justified up to the mildly nonlinear regime. However, it may not be valid in the fully nonlinear regime, especially at smaller scales, where the fluctuations grow $\Delta_\rho \gg 1$. In order to treat the smaller scales properly, we need to improve LTA in our future study. We would like to report the analysis on these issues in the near future.

ACKNOWLEDGMENTS

We would like to thank Paul Haines, Hiraku Mutoh, Kamilla Piotrkowska, Naoshi Sugiyama, Takayuki Tatekawa, and Kenji Tomita for many useful discussions. This work was supported partially by a Grant-in-Aid for Scientific Research Fund of the Ministry of Education, Science and Culture (Specially Promoted Research Grant No. 08102010), and by a Waseda University Grant for Special Research Projects.

APPENDIX A: THE BASIC EQUATIONS FOR THE CASE WITH FLUCTUATIONS

To be complete, here, we present a full set of our basic equations, which have been used in our renormalization analysis for Newtonian cosmology. Those include fluctuations up to second order cumulants as well as shear and tidal forces.

1. The RG equations for averaged variables

$$\frac{d\langle\rho\rangle}{dl}=\mathcal{S}[\langle\theta\rangle-2]\langle\rho\rangle, \tag{A1}$$

$$\frac{d\langle\theta\rangle}{dl}=\mathcal{S}\left[\left(\frac{1}{3}\langle\theta\rangle-1\right)\langle\theta\rangle+4\pi G\langle\rho\rangle+6(\langle\sigma_+\rangle^2+\langle\sigma_-\rangle^2)-\frac{2}{3}\langle\theta^2\rangle_c+6(\langle\sigma_+^2\rangle_c+\langle\sigma_-^2\rangle_c)\right], \tag{A2}$$

$$\frac{d\langle\sigma_+\rangle}{dl}=\mathcal{S}\left[\left(\frac{2}{3}\langle\theta\rangle-1\right)\langle\sigma_+\rangle-\langle\sigma_+\rangle^2+\langle\sigma_-\rangle^2+\langle E_+\rangle-\frac{1}{3}\langle\theta\sigma_+\rangle_c-\langle\sigma_+^2\rangle_c+\langle\sigma_-^2\rangle_c\right], \tag{A3}$$

$$\frac{d\langle\sigma_-\rangle}{dl}=\mathcal{S}\left[\left(\frac{2}{3}\langle\theta\rangle-1\right)\langle\sigma_-\rangle+2\langle\sigma_+\rangle\langle\sigma_-\rangle+\langle E_-\rangle-\frac{1}{3}\langle\theta\sigma_-\rangle_c+2\langle\sigma_+\sigma_-\rangle_c\right], \tag{A4}$$

$$\frac{d\langle E_+\rangle}{dl}=\mathcal{S}[(\langle\theta\rangle-2)\langle E_+\rangle+4\pi G\langle\rho\rangle\langle\sigma_+\rangle+4\pi G\langle\rho\sigma_+\rangle_c], \tag{A5}$$

$$\frac{d\langle E_-\rangle}{dl}=\mathcal{S}[(\langle\theta\rangle-2)\langle E_-\rangle+4\pi G\langle\rho\rangle\langle\sigma_-\rangle+4\pi G\langle\rho\sigma_-\rangle_c]. \tag{A6}$$

2. The RG equations for second order cumulants

$$\frac{d\langle\rho^2\rangle_c}{dl}=2\mathcal{S}[(\langle\theta\rangle-2)\langle\rho^2\rangle_c+\langle\rho\rangle\langle\rho\theta\rangle_c], \tag{A7}$$

$$\frac{d\langle\theta^2\rangle_c}{dl}=2\mathcal{S}\left[\left(\frac{2}{3}\langle\theta\rangle-1\right)\langle\theta^2\rangle_c+4\pi G\langle\rho\theta\rangle_c+12(\langle\sigma_+\rangle\langle\theta\sigma_+\rangle_c+\langle\sigma_-\rangle\langle\theta\sigma_-\rangle_c)\right], \tag{A8}$$

$$\frac{d\langle\rho\theta\rangle_c}{dl}=\mathcal{S}\left[\left(\frac{5}{3}\langle\theta\rangle-3\right)\langle\rho\theta\rangle_c+4\pi G\langle\rho^2\rangle_c+\langle\rho\rangle\langle\theta^2\rangle_c+12(\langle\sigma_+\rangle\langle\rho\sigma_+\rangle_c+\langle\sigma_-\rangle\langle\rho\sigma_-\rangle_c)\right], \tag{A9}$$

$$\frac{d\langle\rho\sigma_+\rangle_c}{dl}=\mathcal{S}\left[\left(\frac{5}{3}\langle\theta\rangle-2\langle\sigma_+\rangle-3\right)\langle\rho\sigma_+\rangle_c+2\langle\sigma_-\rangle\langle\rho\sigma_-\rangle_c+\frac{2}{3}\langle\sigma_+\rangle\langle\rho\theta\rangle_c+\langle\rho\rangle\langle\theta\sigma_+\rangle_c+\langle\rho E_+\rangle_c\right], \tag{A10}$$

$$\frac{d\langle\rho\sigma_-\rangle_c}{dl}=\mathcal{S}\left[\left(\frac{5}{3}\langle\theta\rangle+2\langle\sigma_+\rangle-3\right)\langle\rho\sigma_-\rangle_c+2\langle\sigma_-\rangle\langle\rho\sigma_+\rangle_c+\frac{2}{3}\langle\sigma_-\rangle\langle\rho\theta\rangle_c+\langle\rho\rangle\langle\theta\sigma_-\rangle_c+\langle\rho E_-\rangle_c\right], \tag{A11}$$

$$\frac{d\langle\rho E_+\rangle_c}{dl}=\mathcal{S}[2(\langle\theta\rangle-2)\langle\rho E_+\rangle_c+\langle E_+\rangle\langle\rho\theta\rangle_c+\langle\rho\rangle\langle\theta E_+\rangle_c+4\pi G(\langle\sigma_+\rangle\langle\rho^2\rangle_c+\langle\rho\rangle\langle\rho\sigma_+\rangle_c)], \tag{A12}$$

$$\frac{d\langle\rho E_-\rangle_c}{dl}=\mathcal{S}[2(\langle\theta\rangle-2)\langle\rho E_-\rangle_c+\langle E_-\rangle\langle\rho\theta\rangle_c+\langle\rho\rangle\langle\theta E_-\rangle_c+4\pi G(\langle\sigma_-\rangle\langle\rho^2\rangle_c+\langle\rho\rangle\langle\rho\sigma_-\rangle_c)], \tag{A13}$$

$$\begin{aligned}\frac{d\langle\theta\sigma_+\rangle_c}{dl}=\mathcal{S}\Bigg[&2\left(\frac{2}{3}\langle\theta\rangle-\langle\sigma_+\rangle-1\right)\langle\theta\sigma_+\rangle_c+2\langle\sigma_-\rangle\langle\theta\sigma_-\rangle_c+\frac{2}{3}\langle\sigma_+\rangle\langle\theta^2\rangle_c+\langle\theta E_+\rangle_c+4\pi G\langle\rho\sigma_+\rangle_c\\&+12(\langle\sigma_+\rangle\langle\sigma_+^2\rangle_c+\langle\sigma_-\rangle\langle\sigma_+\sigma_-\rangle_c)\Bigg],\end{aligned} \tag{A14}$$

$$\begin{aligned}\frac{d\langle\theta\sigma_-\rangle_c}{dl}=\mathcal{S}\Bigg[&2\left(\frac{2}{3}\langle\theta\rangle+\langle\sigma_+\rangle-1\right)\langle\theta\sigma_-\rangle_c+2\langle\sigma_-\rangle\langle\theta\sigma_+\rangle_c+\frac{2}{3}\langle\sigma_-\rangle\langle\theta^2\rangle_c+\langle\theta E_-\rangle_c+4\pi G\langle\rho\sigma_-\rangle_c\\&+12(\langle\sigma_-\rangle\langle\sigma_-^2\rangle_c+\langle\sigma_+\rangle\langle\sigma_+\sigma_-\rangle_c)\Bigg],\end{aligned} \tag{A15}$$

$$\frac{d\langle \theta E_+\rangle_c}{dl}=\mathcal{S}\Bigg[\left(\frac{5}{3}\langle\theta\rangle-3\right)\langle\theta E_+\rangle_c+\langle E_+\rangle\langle\theta^2\rangle_c+4\pi G(\langle\rho\rangle\langle\theta\sigma_+\rangle_c+\langle\sigma_+\rangle\langle\rho\theta\rangle_c+\langle\rho E_+\rangle_c)$$
$$+12(\langle\sigma_+\rangle\langle\sigma_+E_+\rangle_c+\langle\sigma_-\rangle\langle\sigma_-E_+\rangle_c)\Bigg], \tag{A16}$$

$$\frac{d\langle \theta E_-\rangle_c}{dl}=\mathcal{S}\Bigg[\left(\frac{5}{3}\langle\theta\rangle-3\right)\langle\theta E_-\rangle_c+\langle E_-\rangle\langle\theta^2\rangle_c+4\pi G(\langle\rho\rangle\langle\theta\sigma_-\rangle_c+\langle\sigma_-\rangle\langle\rho\theta\rangle_c+\langle\rho E_-\rangle_c)$$
$$+12(\langle\sigma_+\rangle\langle\sigma_+E_-\rangle_c+\langle\sigma_-\rangle\langle\sigma_-E_-\rangle_c)\Bigg], \tag{A17}$$

$$\frac{d\langle \sigma_+^2\rangle_c}{dl}=\mathcal{S}\left[2\left(\frac{2}{3}\langle\theta\rangle-2\langle\sigma_+\rangle-1\right)\langle\sigma_+^2\rangle_c+\frac{4}{3}\langle\sigma_+\rangle\langle\theta\sigma_+\rangle_c+4\langle\sigma_-\rangle\langle\sigma_+\sigma_-\rangle_c+2\langle\sigma_+E_+\rangle_c\right], \tag{A18}$$

$$\frac{d\langle \sigma_-^2\rangle_c}{dl}=\mathcal{S}\left[2\left(\frac{2}{3}\langle\theta\rangle+2\langle\sigma_+\rangle-1\right)\langle\sigma_-^2\rangle_c+\frac{4}{3}\langle\sigma_-\rangle\langle\theta\sigma_-\rangle_c+4\langle\sigma_-\rangle\langle\sigma_+\sigma_-\rangle_c+2\langle\sigma_-E_-\rangle_c\right], \tag{A19}$$

$$\frac{d\langle \sigma_+\sigma_-\rangle_c}{dl}=\mathcal{S}\Bigg[2\left(\frac{2}{3}\langle\theta\rangle-1\right)\langle\sigma_+\sigma_-\rangle_c+\frac{2}{3}(\langle\sigma_+\rangle\langle\theta\sigma_-\rangle_c+\langle\sigma_-\rangle\langle\theta\sigma_+\rangle_c)+2\langle\sigma_-\rangle(\langle\sigma_+^2\rangle_c+\langle\sigma_-^2\rangle_c)$$
$$+\langle\sigma_+E_-\rangle_c+\langle\sigma_-E_+\rangle_c\Bigg], \tag{A20}$$

$$\frac{d\langle E_+^2\rangle_c}{dl}=2\mathcal{S}[(\langle\theta\rangle-2)\langle E_+^2\rangle_c+\langle E_+\rangle\langle\theta E_+\rangle_c+4\pi G(\langle\rho\rangle\langle\sigma_+E_+\rangle_c+\langle\sigma_+\rangle\langle\rho E_+\rangle_c)], \tag{A21}$$

$$\frac{d\langle E_-^2\rangle_c}{dl}=2\mathcal{S}[(\langle\theta\rangle-2)\langle E_-^2\rangle_c+\langle E_-\rangle\langle\theta E_-\rangle_c+4\pi G(\langle\rho\rangle\langle\sigma_-E_-\rangle_c+\langle\sigma_-\rangle\langle\rho E_-\rangle_c)], \tag{A22}$$

$$\frac{d\langle E_+E_-\rangle_c}{dl}=\mathcal{S}[2(\langle\theta\rangle-2)\langle E_+E_-\rangle_c+\langle E_-\rangle\langle\theta E_+\rangle_c+\langle E_+\rangle\langle\theta E_-\rangle_c+4\pi G\langle\rho\rangle(\langle\sigma_+E_-\rangle_c+\langle\sigma_-E_+\rangle_c)$$
$$+4\pi G(\langle\sigma_+\rangle\langle\rho E_-\rangle_c+\langle\sigma_-\rangle\langle\rho E_+\rangle_c)], \tag{A23}$$

$$\frac{d\langle \sigma_+E_+\rangle_c}{dl}=\mathcal{S}\Bigg[\left(\frac{5}{3}\langle\theta\rangle-2\langle\sigma_+\rangle-3\right)\langle\sigma_+E_+\rangle_c+2\langle\sigma_-\rangle\langle\sigma_-E_+\rangle_c+\langle E_+\rangle\langle\theta\sigma_+\rangle_c+\langle E_+^2\rangle_c+\frac{2}{3}\langle\sigma_+\rangle\langle\theta E_+\rangle_c$$
$$+4\pi G(\langle\rho\rangle\langle\sigma_+^2\rangle_c+\langle\sigma_+\rangle\langle\rho\sigma_+\rangle_c)\Bigg], \tag{A24}$$

$$\frac{d\langle \sigma_+E_-\rangle_c}{dl}=\mathcal{S}\Bigg[\left(\frac{5}{3}\langle\theta\rangle-2\langle\sigma_+\rangle-3\right)\langle\sigma_+E_-\rangle_c+2\langle\sigma_-\rangle\langle\sigma_-E_-\rangle_c+\langle E_-\rangle\langle\theta\sigma_+\rangle_c+\langle E_+E_-\rangle_c$$
$$+\frac{2}{3}\langle\sigma_+\rangle\langle\theta E_-\rangle_c+4\pi G(\langle\rho\rangle\langle\sigma_+\sigma_-\rangle_c+\langle\sigma_-\rangle\langle\rho\sigma_+\rangle_c)\Bigg], \tag{A25}$$

$$\frac{d\langle \sigma_-E_+\rangle_c}{dl}=\mathcal{S}\Bigg[\left(\frac{5}{3}\langle\theta\rangle+2\langle\sigma_+\rangle-3\right)\langle\sigma_-E_+\rangle_c+2\langle\sigma_-\rangle\langle\sigma_+E_+\rangle_c+\langle E_+\rangle\langle\theta\sigma_-\rangle_c+\langle E_+E_-\rangle_c$$
$$+\frac{2}{3}\langle\sigma_-\rangle\langle\theta E_+\rangle_c+4\pi G(\langle\rho\rangle\langle\sigma_+\sigma_-\rangle_c+\langle\sigma_+\rangle\langle\rho\sigma_-\rangle_c)\Bigg], \tag{A26}$$

$$\frac{d\langle \sigma_-E_-\rangle_c}{dl}=\mathcal{S}\Bigg[\left(\frac{5}{3}\langle\theta\rangle+2\langle\sigma_+\rangle-3\right)\langle\sigma_-E_-\rangle_c+2\langle\sigma_-\rangle\langle\sigma_+E_-\rangle_c+\langle E_-\rangle\langle\theta\sigma_-\rangle_c+\langle E_-^2\rangle_c+\frac{2}{3}\langle\sigma_-\rangle\langle\theta E_-\rangle_c$$
$$+4\pi G(\langle\rho\rangle\langle\sigma_-^2\rangle_c+\langle\sigma_-\rangle\langle\rho\sigma_-\rangle_c)\Bigg]. \tag{A27}$$

[1] G. de Vaucouleurs, Science **167**, 1203 (1970).
[2] P. J. E. Peebles, *The Large-Scale Structure of the Universe* (Princeton University Press, Princeton, NJ, 1980), Chap. IV.
[3] P. H. Coleman and L. Pietronero, Phys. Rep. **213**, 1 (1992); L. Pietronero, M. Montuori, and F. S. Labini, in *Critical Dialogues in Cosmology*, edited by N. Turok (World Scientific, Singapore, 1997).
[4] N. A. Bahcall, L. Lubin, and V. Dorman, Astrophys. J. **447**, L81 (1995); N. A. Bahcall, in *Unsolved Problems in Astrophysics*, edited by J. N. Bahcall and J. P. Ostriker (Princeton University Press, Princeton, NJ, 1997), p. 61.
[5] The parameters H_0, Ω_0 can be found in *Critical Dialogues in Cosmology*, edited by N. Turok (World Scientific, Singapore, 1997), Pt. I.
[6] In the present consideration, we exclude the direct observations of Ω based on the space-time geometry.
[7] R. A. Isaacson, Phys. Rev. **166**, 1272 (1968); T. Futamase, Phys. Rev. Lett. **61**, 2175 (1988); Mon. Not. R. Astron. Soc. **237**, 187 (1989); Prog. Theor. Phys. **89**, 581 (1993); Phys. Rev. D **53**, 681 (1996); R. M. Zalaletdinov, Gen. Relativ. Gravit. **24**, 1015 (1992); gr-qc/9703016; H. Russ, M. H. Soffel, M. Kasai, and G. Börner, Phys. Rev. D **56**, 2044 (1997).
[8] T. Buchert, ''*Mapping, Measuring and Modeling the Universe*,'' edited by P. Coles, V. J. Martinetz, and M.-J. Pons-Bordería, 1996, astro-ph/9512107; T. Buchert and J. Ehlers, Astron. Astrophys. **320**, 1 (1997).
[9] K. G. Wilson and J. Kogut, Phys. Rep. **12**, 76 (1974).
[10] Note added: Recently, we found the paper by H. J. de Vega, N. Sánchez, and F. Combes, astro-ph/9801115, 1998, as one of the examples applying the RG method to cosmology.
[11] T. Koike, T. Hara, and S. Adachi, Phys. Rev. Lett. **74**, 5170 (1995).
[12] T. Hara, T. Koike, and S. Adachi, gr-qc/9607010, 1996; O. Iguchi, A. Hosoya, and T. Koike, Phys. Rev. D **57**, 3340 (1998).
[13] M. Carfora and A. Marzuoli, Phys. Rev. Lett. **53**, 2445 (1984).
[14] M. Carfora and K. Piotrkowska, Phys. Rev. D **52**, 4393 (1995).
[15] E. Bertschinger and A. J. S. Hamilton, Astrophys. J. **435**, 1 (1994).
[16] In this approximation, the third and higher order spatial derivatives are systematically neglected in the equation of motion for the tidal force. This is a generalization of the Zel'dovich approximation, and accuracies of these local approximations are examined for spheroidal configurations by Hui and Bertschinger [17] . It is also worth noticing that the choice of approximation scheme does not change our basic idea in this paper and many of them give similar results.
[17] L. Hui and E. Bertschinger, Astrophys. J. **471**, 1 (1996); **168**, 399 (1974).
[18] The RG equations are written in terms of a scale parameter l. Then a ''stability'' here does not mean dynamical stability. It means what kind of asymptotic behavior of some averaged variables would be expected when a scale is changed.
[19] Other choices of s are mathematically viable, however, they seem not to provide us any interesting model of the Universe.
[20] Such a similarity solution with $s \neq 1$ is related to ''partial similarity'' [21] or ''kinematic self-similarity'' [22] in general relativity.
[21] K. Tomita, Prog. Theor. Phys. **66**, 2055 (1981); Prog. Theor. Phys. Suppl. **70**, 286 (1981); Gen. Relativ. Gravit. **29**, 815 (1997); J Ponce de Leon, J. Math. Phys. **29**, 2479 (1988); Mon. Not. R. Astron. Soc. **250**, 69 (1991).
[22] A. A. Coley, Class. Quantum Grav. **14**, 87 (1997).
[23] If the structure of the Universe is described by the Rayleigh-Lévy fractal, the higher-order cumulants are given as the three-point correlation function $\zeta_{123} = \frac{1}{2}(\xi_{12}\xi_{23} + \xi_{23}\xi_{31} + \xi_{31}\xi_{12})$ and the four-point correlation function $\eta_{1234} = \frac{1}{4}(\xi_{12}\xi_{23}\xi_{34} + \cdots 12$ terms).
[24] This relation may be true only for the present case without higher-order cumulants.
[25] In this approximation, the magnetic part of the Weyl tensor is neglected.
[26] Here, ''initial'' means $l = 0$, which denotes the largest averaging scale of our Universe ($\sim$ horizon scale).
[27] A. Kogut, G. Hinshaw, and A. J. Banday, Phys. Rev. D **55**, 1901 (1997).
[28] R. Balian and R. Schaeffer, Astron. Astrophys. **220**, 1 (1989); **226**, 374 (1989).
[29] J. D. Barrow and A. R. Liddle, Gen. Relativ. Gravit. **29**, 1503 (1997).
[30] M. Aryal and A. Vilenkin, Phys. Lett. B **199**, 351 (1987).